Norwegian Meteorological Institute
met.no
met.no report

NVE

no. 01/2006 Climate

Snow cover and snow water equivalent in Norway: -current conditions (1961-1990) and scenarios for the future (2071-2100)

Dagrun Vikhamar Schuler, Stein Beldring, Eirik J. Førland,
Lars A. Roald and Torill Engen Skaugen

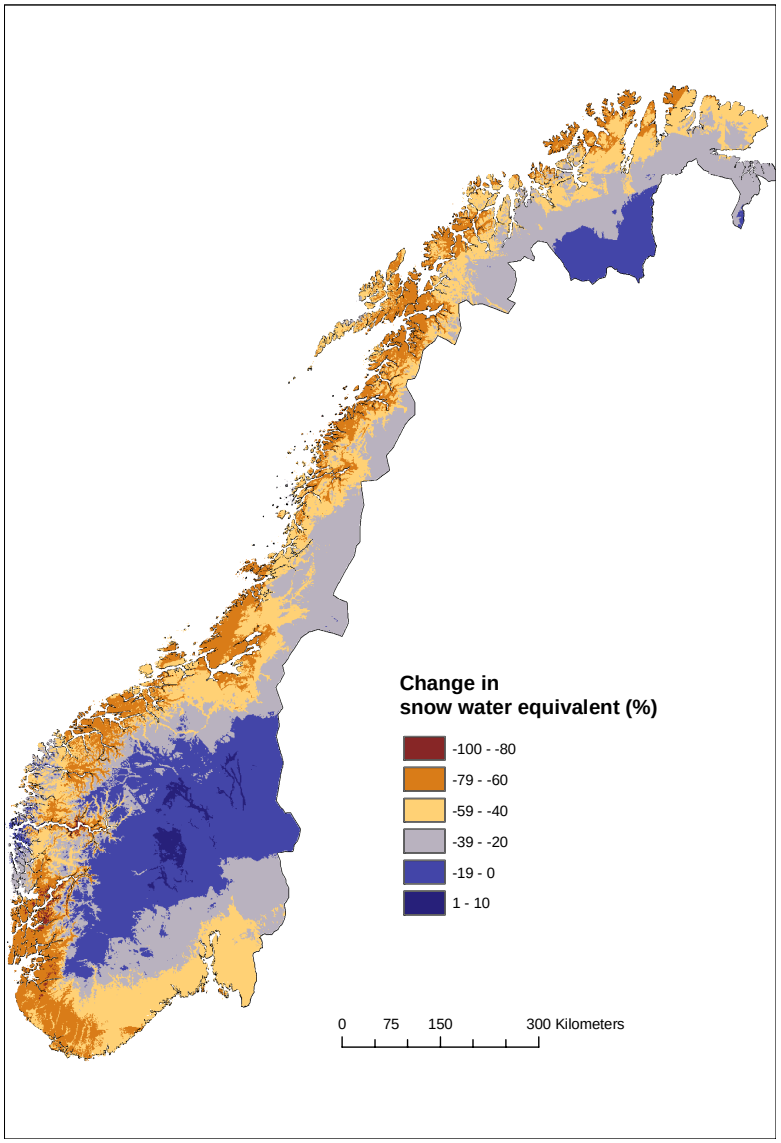

Norwegian Meteorological Institute
met.no

report

NVE

Title	Date
Snow cover and snow water equivalent in Norway: -current conditions (1961-1990) and scenarios for the future 2071-2100)	18th January 2006
Section Climate	**Report no.** no. 01/2006
Author(s) Dagrun Vikhamar Schuler[1], Stein Beldring[2], Eirik J. Førland[1], Lars A. Roald[2] and Torill Engen Skaugen[1] [1]Norwegian Meteorological Institute, [2] Norwegian Water Resources and Energy Directorate.	**Classification** ● Free ○ Restricted **ISSN 1503-8025** **e-ISSN 1503-8025**
Client(s) EBL-Kompetanse A/S (Project: Climate development: consequences for discharge, environment and hydropower production.)	**Client's reference**

Abstract

This report presents projected changes in snow conditions in Norway. Possible changes from present climate (1961-1990) to future climate (2071-2100) are described. Projected air temperature and precipitation data from two climate models (HadAm3 and ECHAM4/OPYC3) run with the B2 emission scenario were dynamically downscaled using the regional climate model HIRHAM, and also locally adjusted to stations in Norway. The Gridded Water Balance model was run using these daily data sets. Snow water equivalent, which is reported in this study, is one of the output variables.

It is found that both the mean annual maximum snow water equivalent and the duration of the snow season are projected to decrease almost everywhere in Norway. Generally, the decrease gets smaller with increasing altitude and distance from the coast. The start of the snow accumulation season is projected approximately 3-4 weeks later than in the present climate. The snow melt season starts earlier, leading to an earlier end of the snow season (approximately 1-7 weeks earlier). Maximum amounts of snow is projected to shift from April/May to March/April. In extreme years the maximum snow water equivalent might be higher than today in a few high altitude or northern drainage basins.

Keywords

Snow cover, snow water equivalent, snow season duration, climate change, Norway

Disciplinary signature	Responsible signature
Eirik J. Førland	Cecilie Mauritzen

Postal address P.O Box 43 Blindern N-0313 OSLO Norway | **Office** Niels Henrik Abels vei 40 | **Telephone** +47 2296 3000 | **Telefax** +47 2296 3050 | **e-mail:** met.inst@met.no **Internet:** met.no | **Bank account** 7694 05 00601 | **Swift code** DNBANOKK

Contents

1 Introduction

Global warming of the surface temperature with approximately 0.6°C has been observed the last 100 years (Folland et al., 2001). Different emission scenarios project a further increase of global temperature between 1°C to 5°C (Cubasch et al., 2001). Globally averaged water vapour concentrations, evaporation and precipitation are projected to increase. At regional scale both increases and decreases in precipitation are projected. The projections of the development of precipitation, however, are even more uncertain than for temperature (Benestad, 2002).

This report presents projected changes in snow conditions for the entire Norwegian mainland and in detail for 12 Norwegian drainage basins. The report summarises possible changes in snow water equivalent, time development of the snow cover and snow season duration including start and end of the snow season. The presented snow conditions result from running a hydrological model with projected temperature and precipitation as input climate variables.

The report is divided into five Chapters. Chapter 2 gives an overview of the dataset and the hydrological model used in the analysis. Countrywide maps of annual maximum snow water equivalent and number of days with snow for current (1961-1990) and future climate (2071-2100) are presented in Chapter 3. Chapter 4 describes the location and the characteristics of the 12 drainage basins analyzed in the study, as well as snow conditions for current climate (1961-1990) and snow conditions projected for future climate (2071-2100). The results and uncertainties regarding the analysis are discussed in Chapter 5. A summary is provided in the end of the report. The report is a part of the study "Climate Change and Energy Production Potential" funded by EBL kompetanse AS.

2 Dataset and methods

2.1 GWB Model

The snow statistics presented in this report result from running the Gridded Water Balance (GWB) model (Sælthun, 1996; Beldring et al., 2002, 2003). The GWB model is a spatially distributed version of the HBV model (Bergström, 1976), giving quantitative estimates of hydrological processes in Nordic environments. The water balance is calculated in each grid cell (1 km $\times$ 1 km). The land cover within each grid cell is described with a maximum of four land-cover elements: two vegetation types, glacier area and lake area. The GWB model contains submodules for snow accumulation, snow melt, glacier mass balance, interception storage, soil moisture storage, evapotranspiration, ground water storage, lake evaporation and runoff response. Both snow accumulation and snow melt are modeled on sub-grid scale. Snow is accumulated by assuming a lognormal distribution of snow for each grid cell, where the coefficient of variation is a function of land-cover type. In doing so, differences in even and uneven snow distribution in mountain areas, forests and lowland areas are taken into account. Snow melt is modelled using a temperature index approach (degree-day model), where the melt factor determines the amount of snow melt when the temperature exceeds a specified threshold.

The GWB model is run using daily time steps. Therefore, daily values for precipitation and temperature is necessary model input. Usually, temperature and precipitation are estimated for each grid cell using inverse distance weighting of the three nearest precipitation stations and the two nearest temperature stations. The output from the model are daily values of water balance elements such as evaporation, runoff, glacier mass balance and snow water equivalent.

A regionally applicable set of parameters was determined by calibrating the model with the restriction that the same parameter values are used for all computational elements of the model that fall into the same class for land surface properties (Beldring et al., 2003). This calibration procedure rests on the hypothesis that model elements with identical landscape characteristics have similar hydrological behaviour, and should consequently be assigned the same parameter values. The grid cells should represent the significant and systematic variations in the properties of the land surface, and representative (typical) parameter values must be applied for different classes of soil and vegetation types, lakes and glaciers (Gottschalk et al., 2001). The model was calibrated using available information about climate and hydrological processes from all gauged basins in Norway with reliable observations, and parameter values

were transferred to other basins based on the classification of landscape characteristics. Several automatic calibration procedures, which use an optimization algorithm to find those values of model parameters that minimize or maximize, as appropriate, an objective function or statistic of the residuals between model simulated output and observed watershed output, have been developed. The nonlinear parameter estimation method PEST (Doherty et al., 1998) was used in this study. PEST adjusts the parameters of a model between specified lower and upper bounds until the sum of squares of residuals between selected model outputs and a complementary set of observed data are reduced to a minimum. A multi-criteria calibration strategy was applied, where the residuals between model simulated and observed monthly runoff from several basins located in areas with different runoff regimes and landscape characteristics were considered simultaneously.

Vegetation characteristics such as stand height and leaf area index influence the water balance at different time scales through their control on evapotranspiration, snow accumulation and snow melt (Matheussen et al., 2000). The following land use classes were used for describing the properties of the 1 km^2 landscape elements of the model: (i) areas above the tree line with extremely sparse vegetation, mostly lichens, mosses and grass; (ii) areas above the tree line with grass, heather, shrubs or dwarfed trees; (iii) areas below the tree line with subalpine forests; (iv) lowland areas with coniferous or deciduous forests; and (v) non-forested areas below the tree line. The model was run with specific parameters for each land use class controlling snow processes, interception storage, evapotranspiration and subsurface moisture storage and runoff generation. Lake evaporation and glacier mass balance were controlled by parameters with global values.

In order to have confidence in a hydrological model, its performance must be validated. Model performance is usually evaluated by considering one or more objective statistics or functions of the residuals between model simulated output and observed watershed output. The objective functions used in this study were the Nash-Sutcliffe and bias statistics of the residuals, which have a low correlation (Weglarczyk, 1998). The distributed model was calibrated separately for the individual drainage basins in order to produce the catchment-specific hydrological scenarios. Country-wide simulations were produced using a global parameter set based on the multi-criteria calibration strategy described above. Model performance was very good for the individually calibrated catchments, with values of the Nash-Sutcliffe statistic generally above 0.8 and absolute values of the bias statistic in the range 0-5%.

2.2 Input dataset

Daily values of precipitation and temperature are required input data for the GWB model. In our analysis we have used three data sets of precipitation and temperature (Tab. 1 and 2). Dataset A consists of daily observations of precipitation and temperature from weather stations in met.no's station network (from the period 1961-1990, which is the standard normal period). The datasets B and C are projections of precipiation and temperature, generated through three steps: 1. Climate modelling; 2. Dynamical downscaling of the climate scenarios; and 3. Adjustment of the climate scenarios to local sites.

Dataset	**Observations met.no**
A	1961-1990

Table 1: *Observed precipitation and temperature from met.no's station network.*

Dataset	**Climate model**	**Emission scenario**	**Control period**	**Scenario period**
B	HadAm3	B2	1961-1990	2071-2100
C	ECHAM4/OPYC3	B2	1961-1990	2071-2100

Table 2: *Estimated precipitation and temperature from two climate models run with the B2 emission scenario.*

2.2.1 Climate modelling

Global climate scenarios of temperature and precipitation are produced from Atmospheric-Ocean General Circulation Models (AOGCMs). The AOGCMs are run using different emission scenarios. In our analysis two AOGCMs have been used (Tab. 2): 1. The ECHAM4/OPYC3 model from the Max Planck Institute for Meteorology in Germany (Roeckner et al., 1999) and; 2. The HadAm3 from the Hadley Centre for Climate Prediction and Research in United Kingdom (Gordon et al., 2000). Both models are run with the emission scenario B2 (Cubasch et al., 2001), for control periods and scenario periods as specified in Tab. 2. The B2 scenario was selected because it resembles the A1b scenario which will be included in the next IPCC report. Up to 2100 the B2 scenario gives approximately 2.5°C increase in the global temperature. The spatial resolution of the forcing data from the two AOGCMs is approximately 300 km $\times$ 300 km and the temporal resolution is 6 hours.

2.2.2 Dynamical downscaling

To improve the climate simulations to conditions in specific regions in Norway, dynamic downscaling with the regional climate model HIRHAM was performed (Haugen and Iversen, 2005; Bjørge et al., 2000). HIRHAM is based on the physics of ECHAM4 and the dynamics of the weather forecast model HIRLAM (High Resolution Limited Area Model), which is operationally used at met.no. HIRHAM produces climate variables with approximately 55 km $\times$ 55 km spatial resolution every 6 hours.

2.2.3 Local adjustment

The temperature and precipitation data resulting from the HIRHAM model are spatially too coarse for being used as input to the GWB model. An additional adjustment to local stations was necessary. The methods applied for the local adjustment are described in Engen-Skaugen et al. (2002) and Engen-Skaugen (2002).

The adjustment accounts for e.g. differences in station altitude and HIRHAM grid point altitude and the overestimation of precipitation from the HIRHAM model on days without precipitation (Frei et al., 2003). In general, the climate simulations include natural variations of the climate. The simulations for the control period are therefore not directly comparable to station observations on a day-by-day basis. However, the statistical properties of the simulated temperature and precipitation should be similar to those of the observed temperature and precipitation. The local adjustment methods try to maintain these statistical properties (e.g. monthly mean and variance of daily values)

2.3 Output dataset

The GWB produces different water balance elements as output data. In this report only the snow variables are presented. Other results from running the GWB model with the same input datasets are reported in Roald et al. (2006).

The GWB model has been run for the entire mainland Norway, resulting in countrywide maps of 1 km $\times$ 1 km. Additionally, results are presented for 12 drainage basins. The reported snow variables are:

- Maximum snow water equivalent.
- Number of days per year with snow.
- First date of permanent snow cover.
- Last date of permanent snow cover.
- Date of maximum snow water equivalent.

Statistical properties of these variables are calculated from datasets A, B and C (Tab. 1 and 2), and presented as maps, graphs and tables in Chapter 3 and 4. National maps are presented in Chapter 3, while statistics for the 12 drainage basins are presented in Chapter 4.

3 National snow maps

3.1 Current climate (1961-1990)

In this section we present results from running the GWB model using interpolated values of precipitation and temperature based on observations from met.no's station network (data set A in Tab. 1). Two statistically derived national maps are shown (1 km $\times$ 1 km grid cells):

- Mean annual maximum snow water equivalent (mm) (Fig 1).
- Mean number of days per year with more than 50% of the ground covered by snow (Fig 2).

The general trend shows that the amount of snow increases with increasing altitude. Least amount of snow (mean annual maximum snow water equivalent < 100 mm) is observed in regions close to the coast, particularly in western parts and eastern parts of South Norway, as well as in some of the large valley bottoms. Largest amount of snow (mean annual maximum snow water equivalent > 3000 mm) occurs in areas with glaciers (e.g. Svartisen, Jostedalsbreen and Folgefonna). The mountainous regions in western parts of South Norway also receive considerable amounts of snow (mean annual maximum snow water equivalent is 2000-3000 mm).

A similar pattern is observed for the snow season duration. The number of days with more than 50% snow coverage is lowest along the coastal regions in South Norway (<75 days). The coast around Haugesund has less than 20-30 days with 50% snow coverage. The highest number of days with more than 50% snow coverage is observed in regions where there are glaciers and/or high mountains (>276 days).

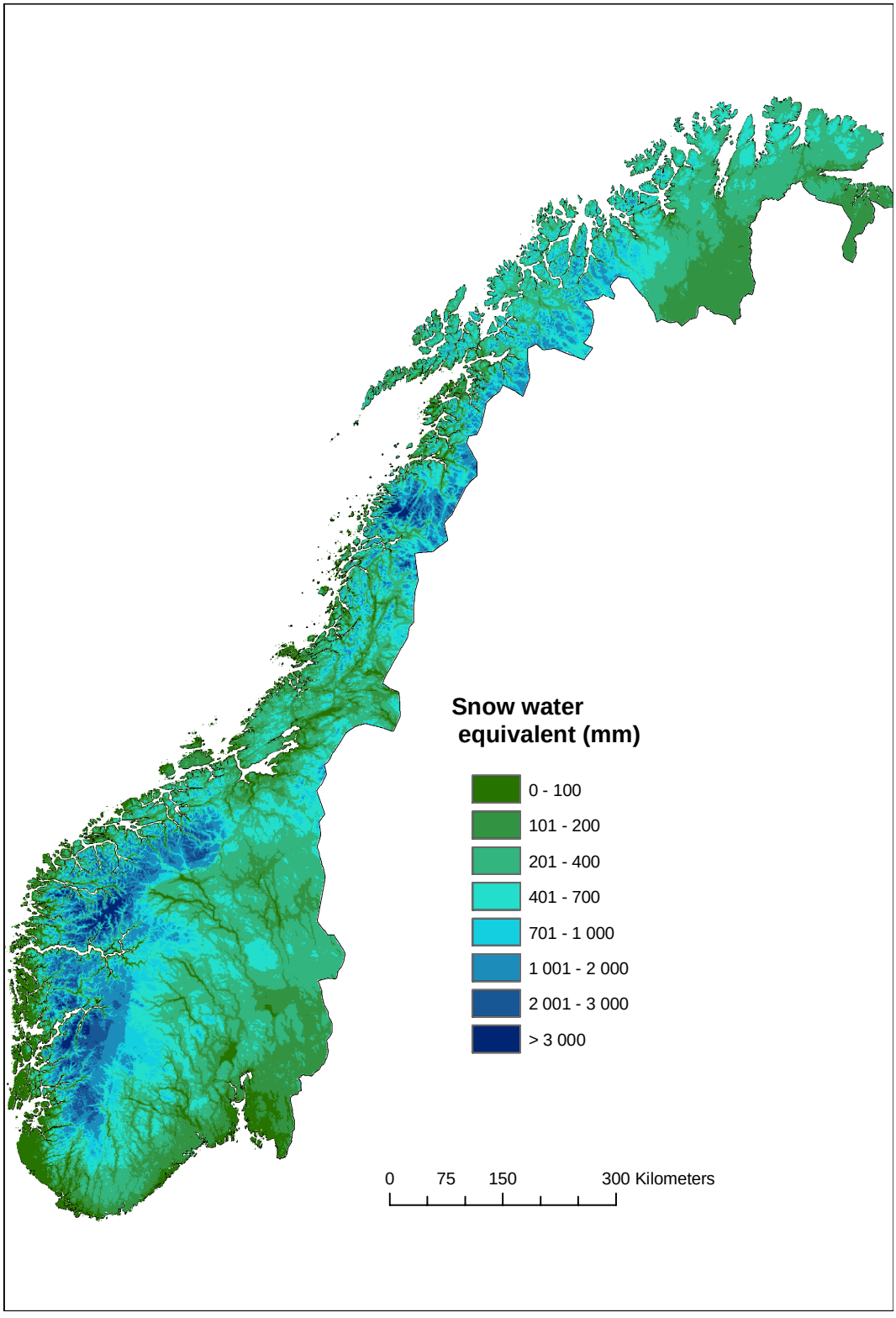

Figure 1: *Mean annual maximum snow water equivalent (mm). Calculated for the period 1961-1990, using precipitation and temperature from met.no's station network (data set A).*

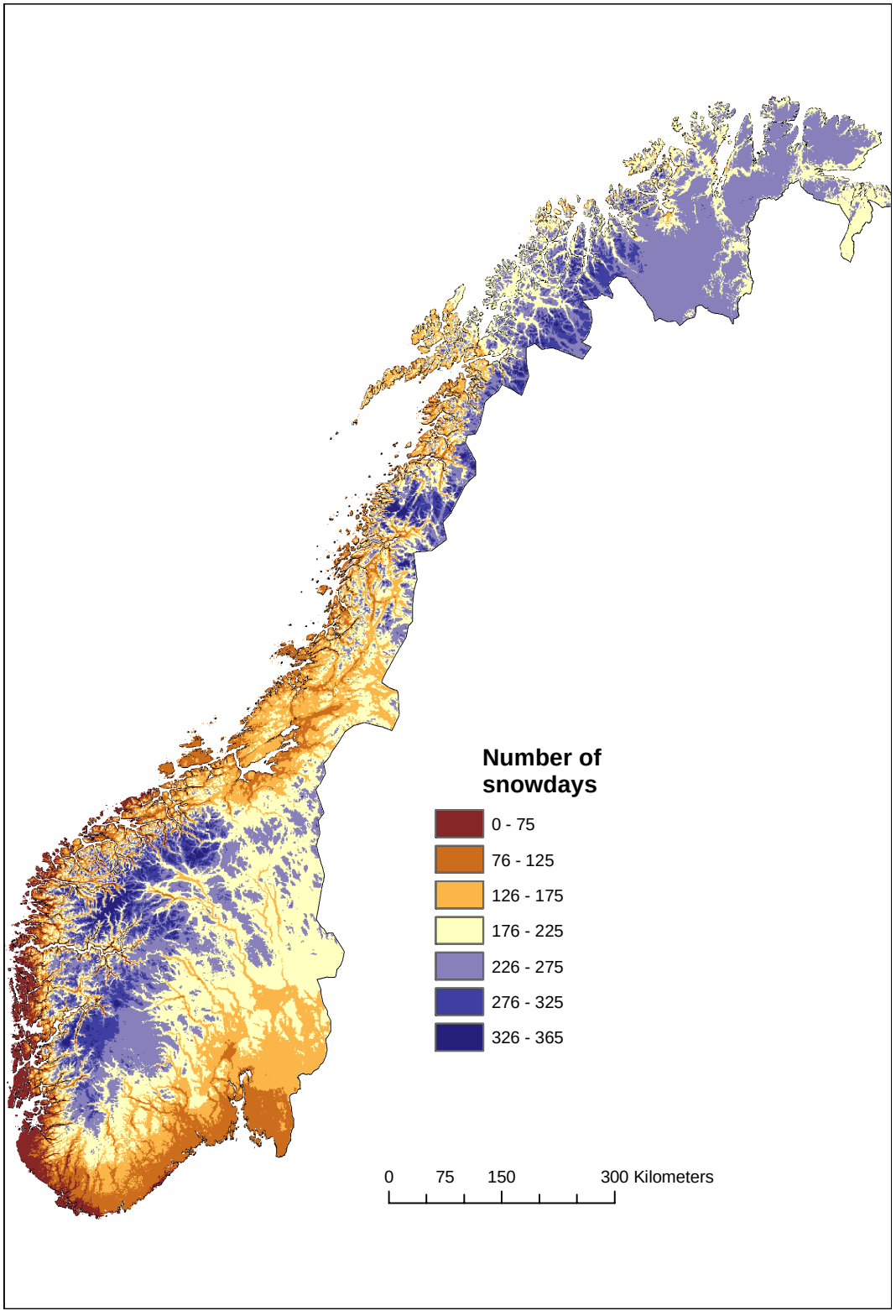

Figure 2: *Mean number of days per year with snow cover > 50%. Calculated for the period 1961-1990, using precipitation and temperature from met.no's station network (data set A).*

3.2 Changes from current (1961-1990) to future climate (2071-2100)

In this section, results from running the GWB model using precipitation and temperature from the two climate models HadAm3 and ECHAM4/OPYC3 are presented (data set B and C in Tab. 2). The GWB model has been run daily for both the control period (1961-1990) and the scenario period (2071-2100). With the use of data from both climate models we present national maps of:

- Change in mean annual snow water equivalent (mm and %) (Figs. 3, 4, 5 and 6).
- Change in mean number of days per year with more than 50% of the ground covered by snow (Figs. 7 and 8).

The absolute change maps (mm) are produced by subtracting the mean values (for each grid cell) of the scenario period (2071-2100) from the mean values (for each grid cell) of the control periods (1961-1990). Percentage change maps show values determined by the equation:
$100 * (scenario - control)/control$.

3.2.1 Mean annual maximum snow water equivalent

We see in the Figs. 3, 4, 5 and 6 that the maximum amounts of snow are projected to decrease almost everywhere in Norway. There are some exceptions. There might be a little increase in amounts of snow in western parts of Finmarksvidda, in some valleys (Gudbrandsdalen: Ringebu, Sør-Fron, Nord-Fron, Sel, Vågå) (Østerdalen: Atna to Tynset) (Rendalen) and Valdres (parts of Øystre Slidre, Vestre Slidre, Nord-Aurdal, Sør-Aurdal and Etnedal). Largest relative changes are expected to occur in some of the outermost areas on the west coast of Norway (80-100% decrease). However, the present snow water equivalent values are low in these areas (<40 mm mean annual maximum snow water equivalent). A north-south zone around the fjords in West-Norway and North-Norway might get decreases up to 60-80%. These areas usually get much autumn precipitation. Smallest relative changes (0-19% decrease) are expected to occur in mountainous areas in South Norway, as well as inner regions of North Norway (Finmarksvidda). The entire snow season will be shorter, and the start of the snow season will be delayed (see the next Section). Precipitation might fall as rain instead of snow. Both climate models ECHAM4/OPYC3 and HadAm3 project similar trends, with some regional differences.

3.2.2 Mean number of days with snow

We see in the Figs. 7 and 8 that the duration of the snow season is projected to be shorter almost everywhere in Norway. The overall pattern shows that this decrease gets smaller with increasing altitude and distance from the coast.

In Northern Norway, the outermost coastal regions get the largest decrease of the length of the snow season, while the innermost regions are expected to get the smallest decreases.

In Southern Norway, the outermost coastal regions are expected to get the smallest decrease in number of days with snow. The current climate show that these areas today also have very short snow season, with less than 75 days with 50% snow coverage (Fig. 2). For the period 2071-2100 the mean snow season duration is projected to be less than 20 days in these regions. A north-south zone around the fjords in West-Norway might get the largest decreases in number of days with snow.

Details about projected changes in the snow season duration for 12 selected drainage basins are presented in Section 4.2.

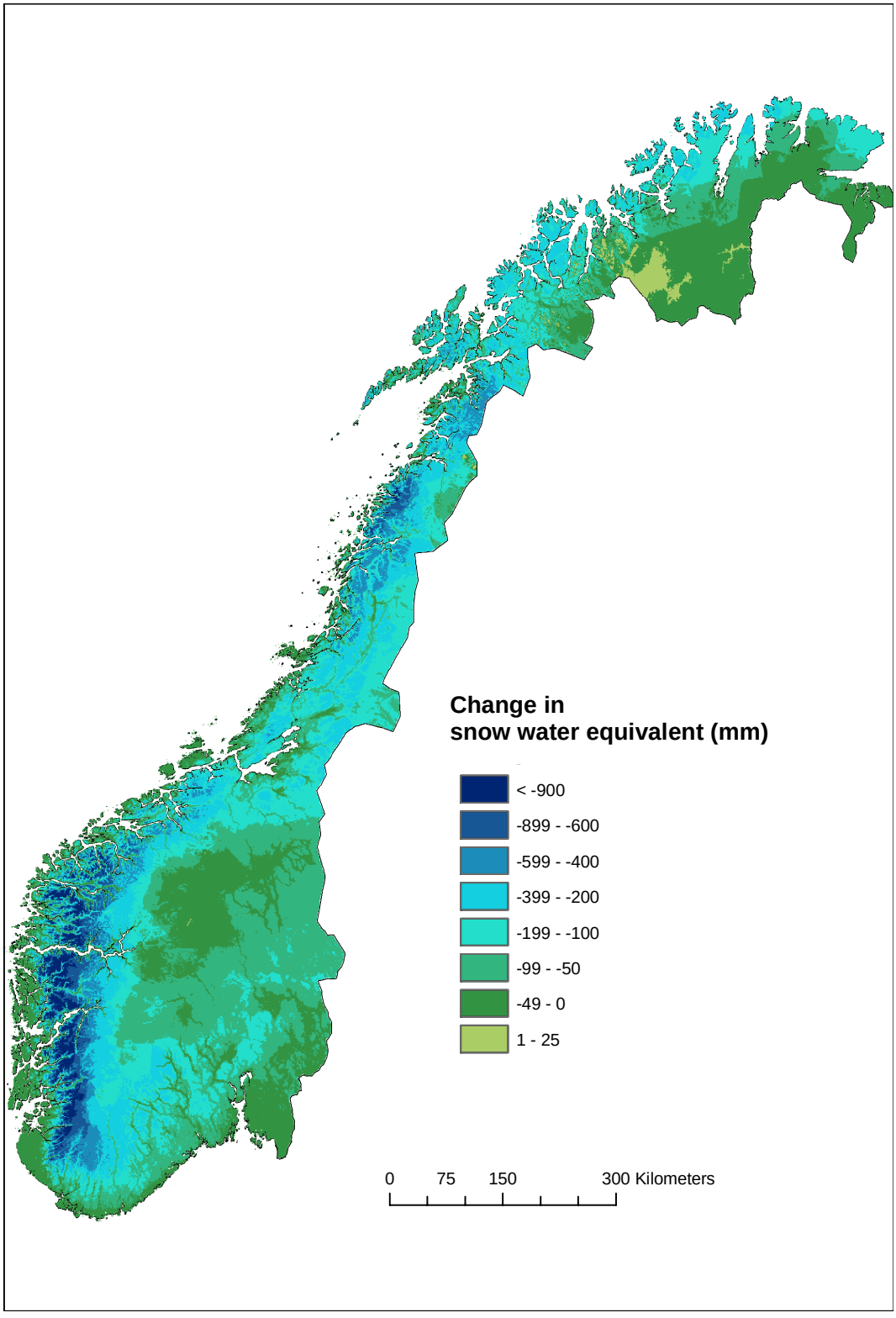

Figure 3: *Change in mean annual maximum snow water equivalent (mm). Calculated difference between the Echam B2 scenario (2071-2100) and the control period (1961-1990).*

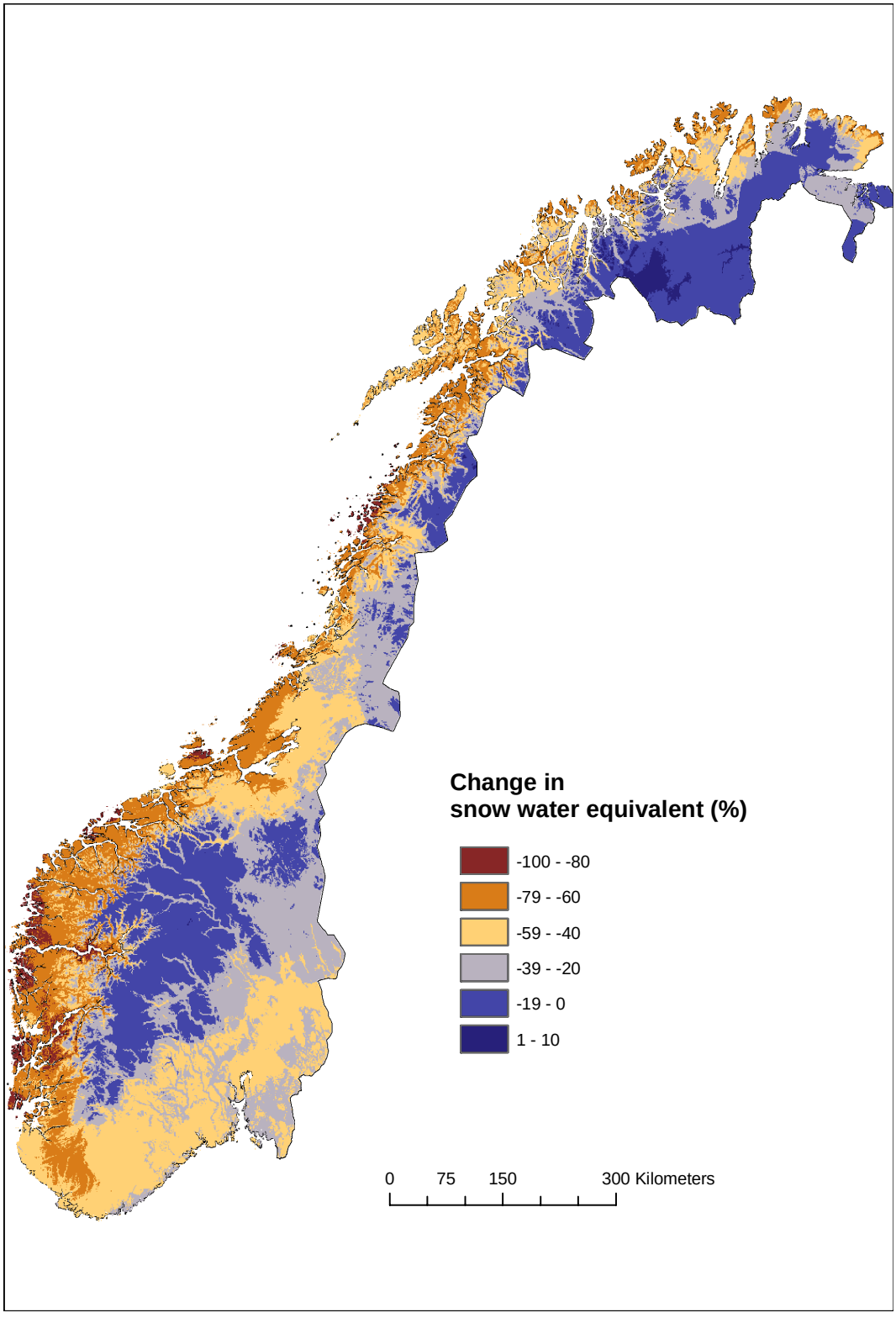

Figure 4: *Change in mean annual maximum snow water equivalent (%). Calculated difference between the Echam B2 scenario (2071-2100) and the control period (1961-1990).*

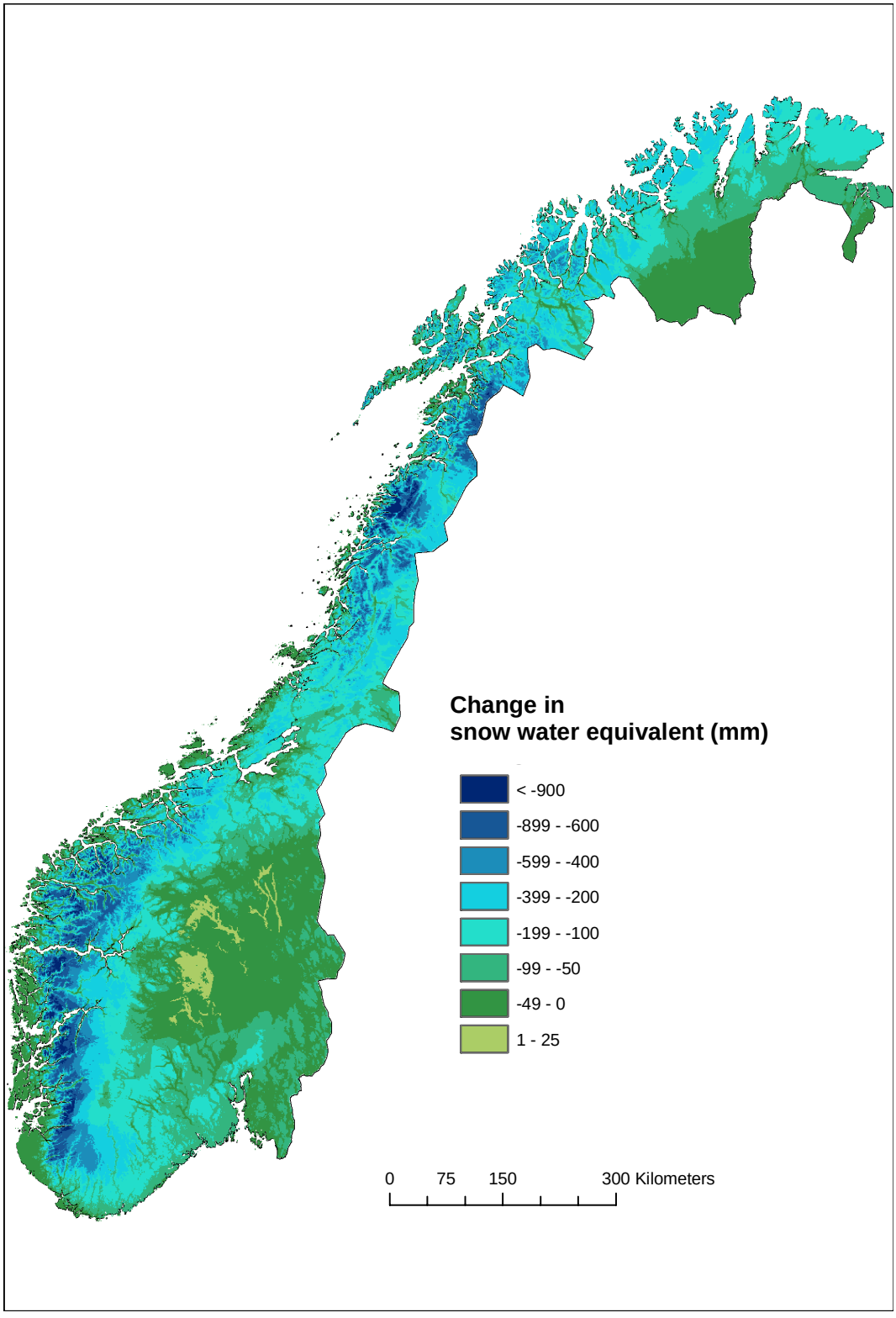

Figure 5: *Change in mean annual maximum snow water equivalent (mm). Calculated difference between the Hadley B2 scenario (2071-2100) and the control period (1961-1990).*

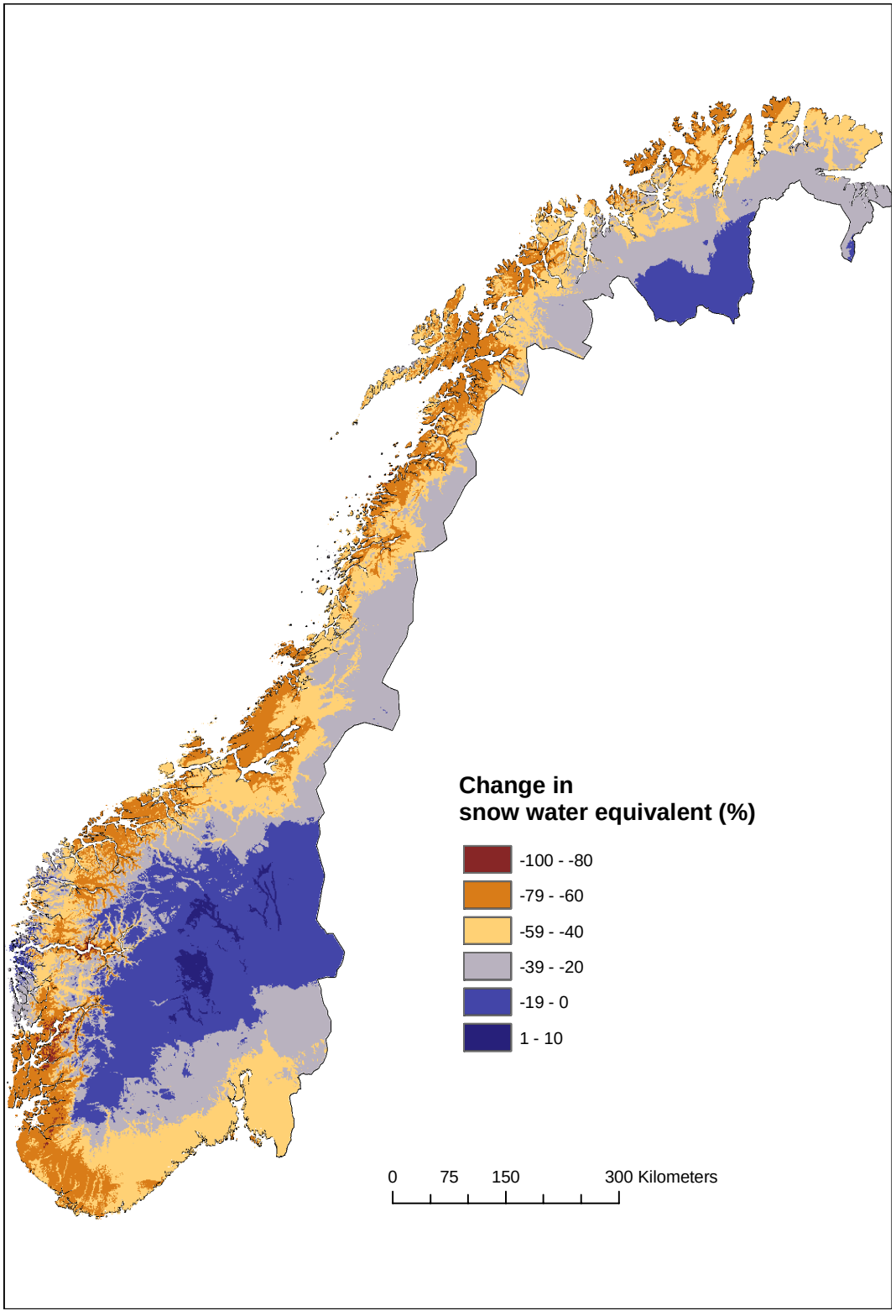

Figure 6: *Change in mean annual maximum snow water equivalent (%). Calculated difference between the Hadley B2 scenario (2071-2100) and the control period (1961-1990).*

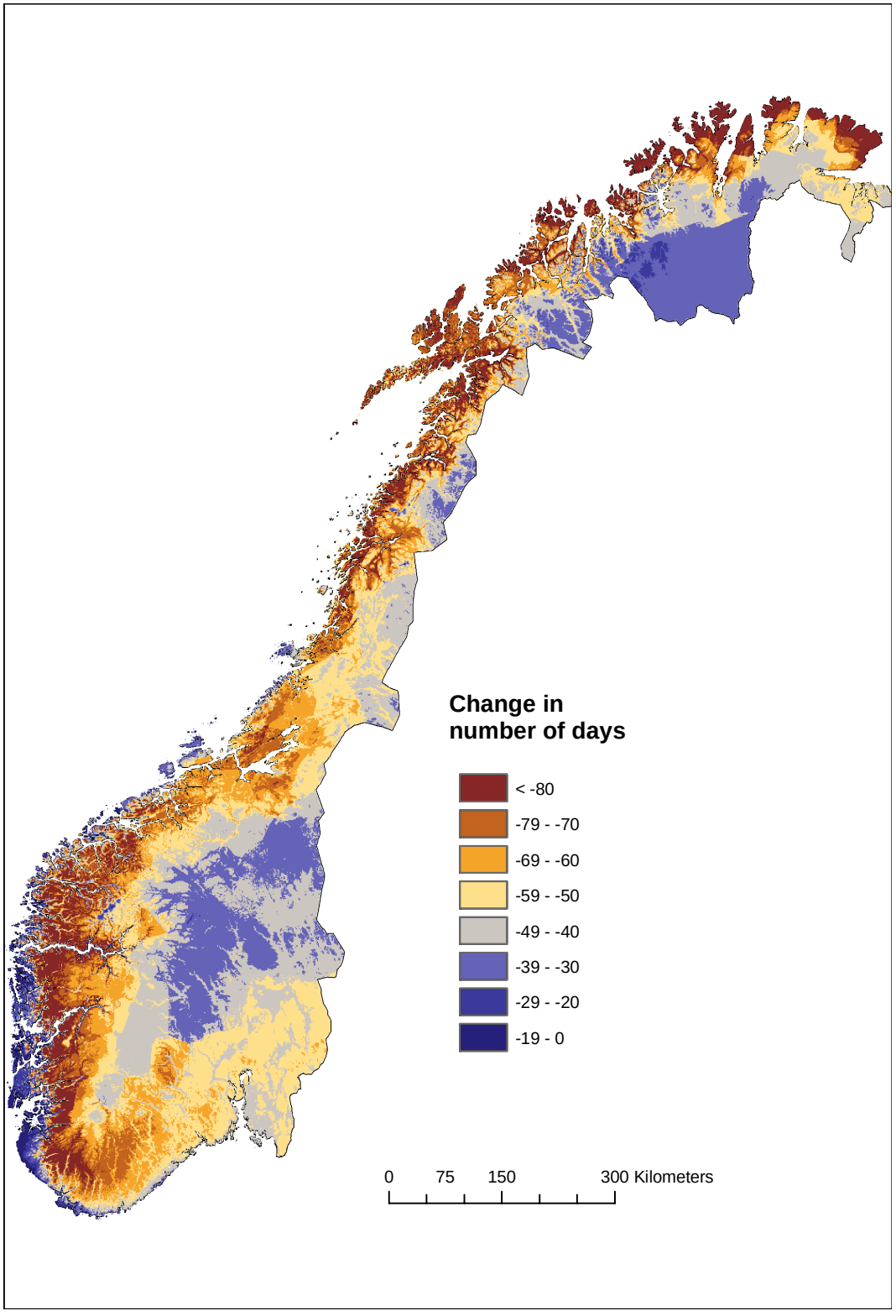

Figure 7: *Change in mean number of days per year with snow cover >50%. Calculated difference between the Echam B2 scenario (2071-2100) and the control period (1961-1990).*

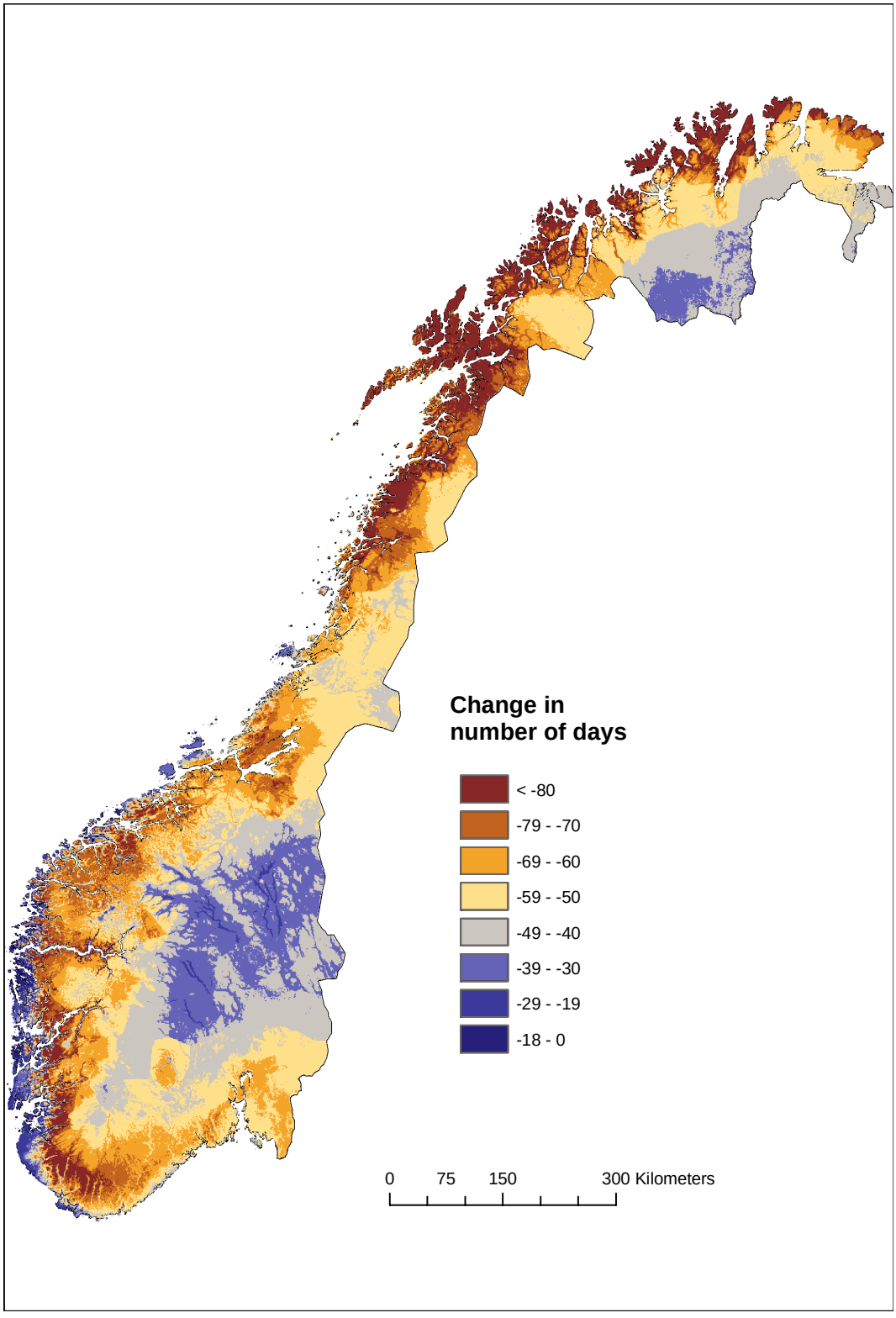

Figure 8: *Change in mean number of days per year with snow cover >50%. Calculated difference between the Hadley B2 scenario (2071-2100) and the control period (1961-1990).*

4 Snow in drainage basins

In this section we present results for 12 selected drainage basins in Norway (Fig 9). Overview of land-cover types, area and elevation for each drainage basin are given in Tabs. 3 and 4.

4.1 Current climate (1961-1990) and future climate (2071-2100)

For each drainage basin we present two graphs showing the time-development of the snow cover during a hydrological year (Figs. 10- 21). Each graph includes minimum, maximum and median curves from both the control period (current climate) and the scenario period (future climate). The graphs to the left represent results using the ECHAM4/OPYC3-B2 data (data set C). The graphs to the right are results from using the HadAm3-B2 data (data set B). Minimum, maximum and median curves have been computed from daily values of snow water equivalent. These daily values represent an average of the snow water equivalent projected to be present within the entire drainage basin, calculated from the 1 km $\times$ 1 km grid cells located within the drainage basin.

On some of the graphs there is a shift in amounts of snow water equivalent from 31 August to 1 September (e.g. Sjodalsvatn). Snow is present until 31 August, while on 1 September there is no snow. The reason for this is obviously not natural variations, but is found in the GWB model. When running the model, the snow storage is set to zero at the start of the hydrological year (1 September) in glacier areas. This is necessary to avoid accumulation of snow on glaciers as the model has no means of converting snow to glacier ice.

Generally, we see that:

- There will be considerably less snow in all the drainage basins, during the entire snow season (see also section 4.3). However, for a few drainage basins (Sjodalsvatn, Orsjoren and Masi) ECHAM4/OPYC3-B2 projects larger amounts of midwinter snow water equivalent in extreme years.
- The snow season becomes shorter, with a later start and an earlier end (see section 4.2)
- Results using the two GCM's with the B2 emission scenario show quite similar snow projections, when comparing the median curves. Minimum and maximum curves show more varying snow projections.

Name	**Elevation (m)**			**Land-cover types (%)**				
	Lowest	**Median**	**Highest**	**Forest**	**Mountain**	**Lake**	**Bog**	**Glacier**
Sjodalsvatn	940	1467	2362	5.3	71.2	9.3	1.0	9.2
Aursunden	685	847	1567	34.0	32.7	12.1	10.0	0
Knappom	170	411	808	78.0	0	1.4	16.5	0
Orsjoren	951	1229	1539	1.6	79.6	12.9	4.6	0
Møsvatn	890	1256	1628	6.0	76.0	12.8	5.0	0.02
Austenå	288	763	1146	61.9	20.3	11.9	5.6	0
Hølen	120	1276	1686	1.9	88.4	0	0.3	0.4
Viksvatn	145	841	1636	22.5	57.3	9.5	1.1	4.7
Risefoss	556	1347	2284	6.8	83.9	1.9	1.2	0.4
Rathe	13	679	1572	37.8	30.2	6.7	14.1	0
Kobbvatn	8	680	1512	15.5	63.1	13.9	0.6	0
Masi	272	451	1085	35.8	1.5	7.0	16.0	0

Table 3: *Land-cover types and elevation statistics for each drainage basin.*

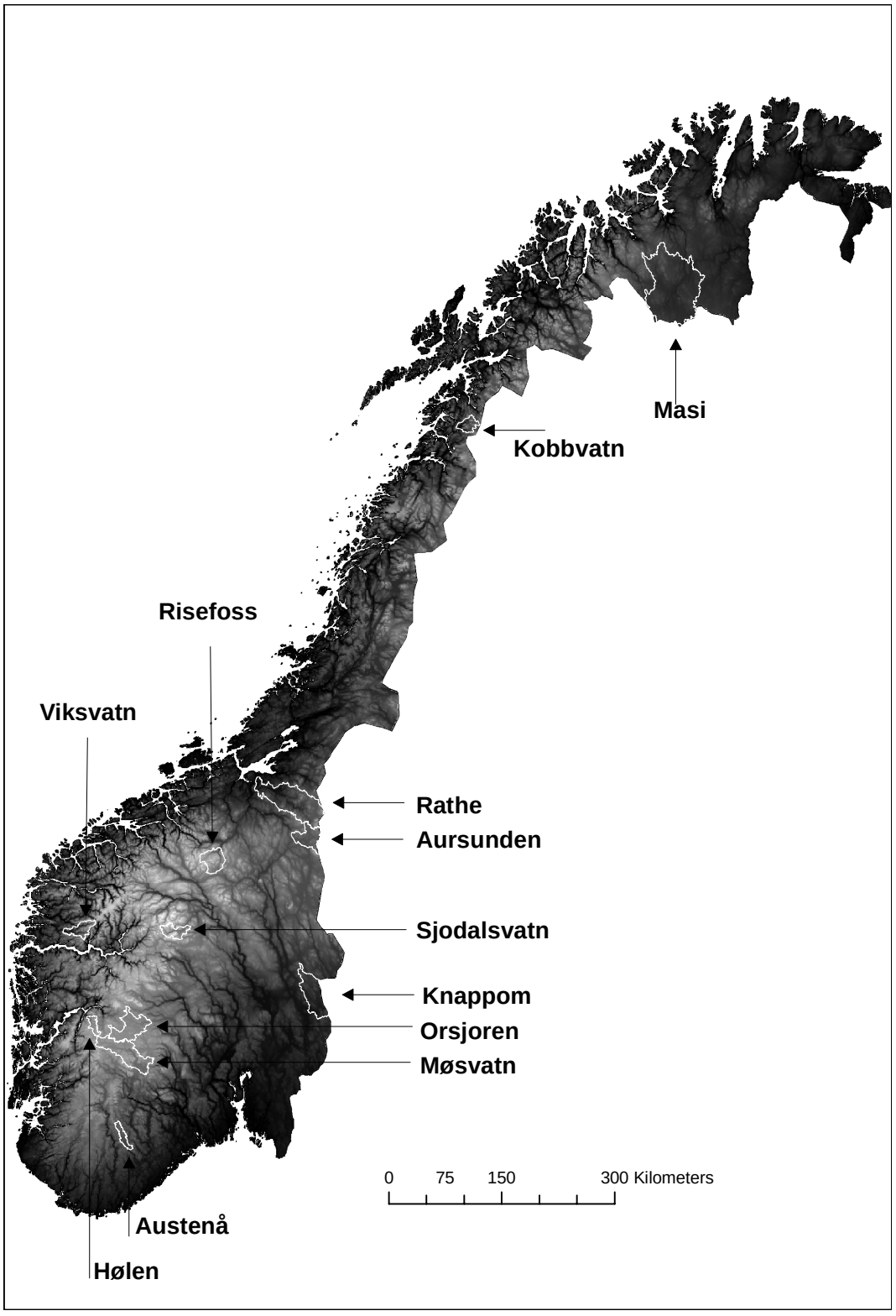

Figure 9: *Map of the drainage basins analyzed in this study. A digital elevation model is shown as background image.*

Name	River	Area (km^2)	Mean annual runoff (mm/year)
Sjodalsvatn	Sjoa	474	1314
Aursunden	Glomma	835	759
Knappom	Flisa	1625	441
Orsjoren	Numedalslågen	1154	839
Møsvatn	Måna	1506	1036
Austenå	Tovdalselv	286	1138
Hølen	Kinso	229	1649
Viksvatn	Gaular	505	2663
Risefoss	Driva	738	681
Rathe	Nidelv	3061	983
Kobbvatn	Kobbelv	386	2012
Masi	Alta	5693	484

Table 4: *drainage basin characteristics.*

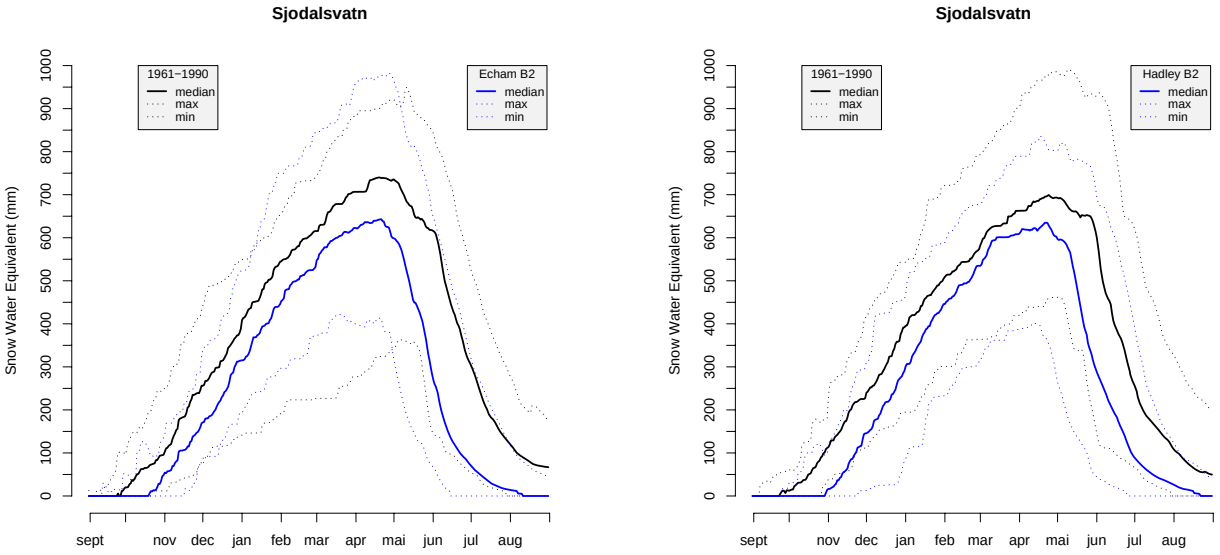

Figure 10: *Daily snow water equivalent: Sjodalsvatn drainage basin*

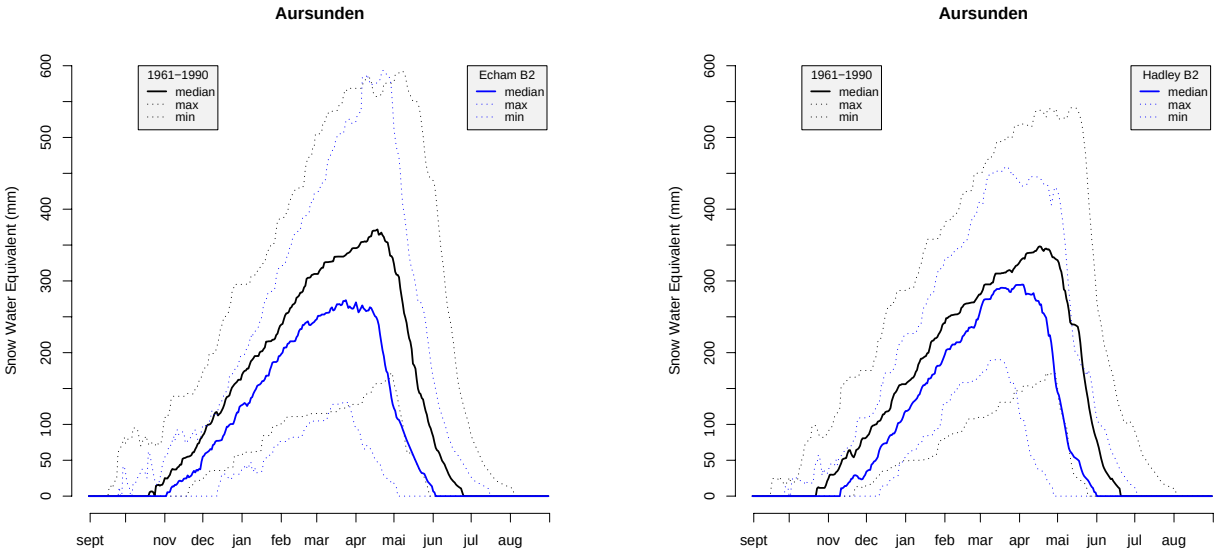

Figure 11: *Daily snow water equivalent: Aursunden drainage basin*

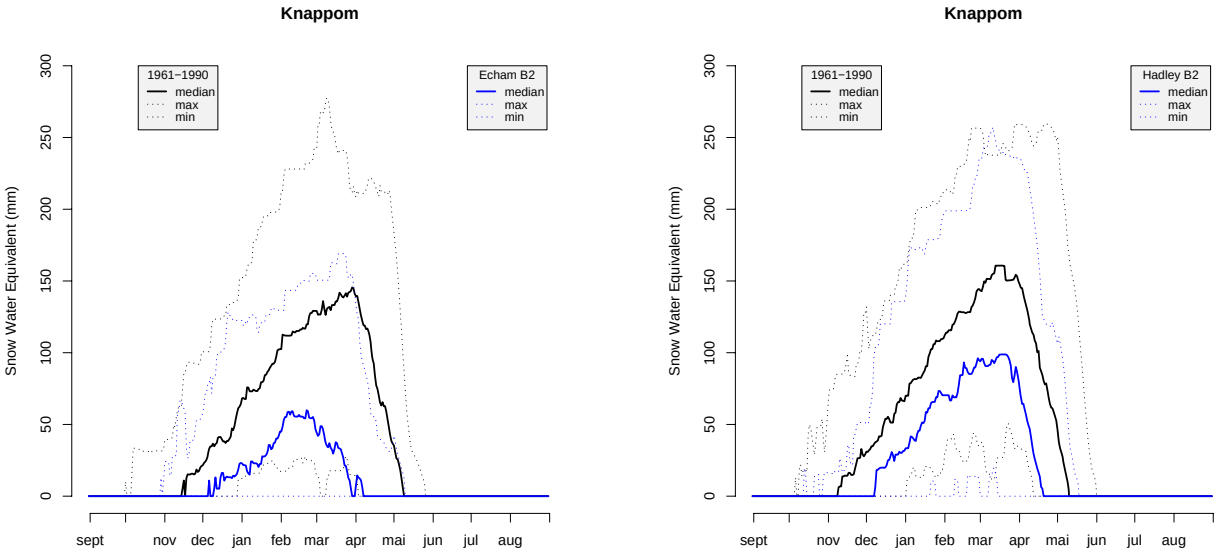

Figure 12: *Daily snow water equivalent: Knappom drainage basin*

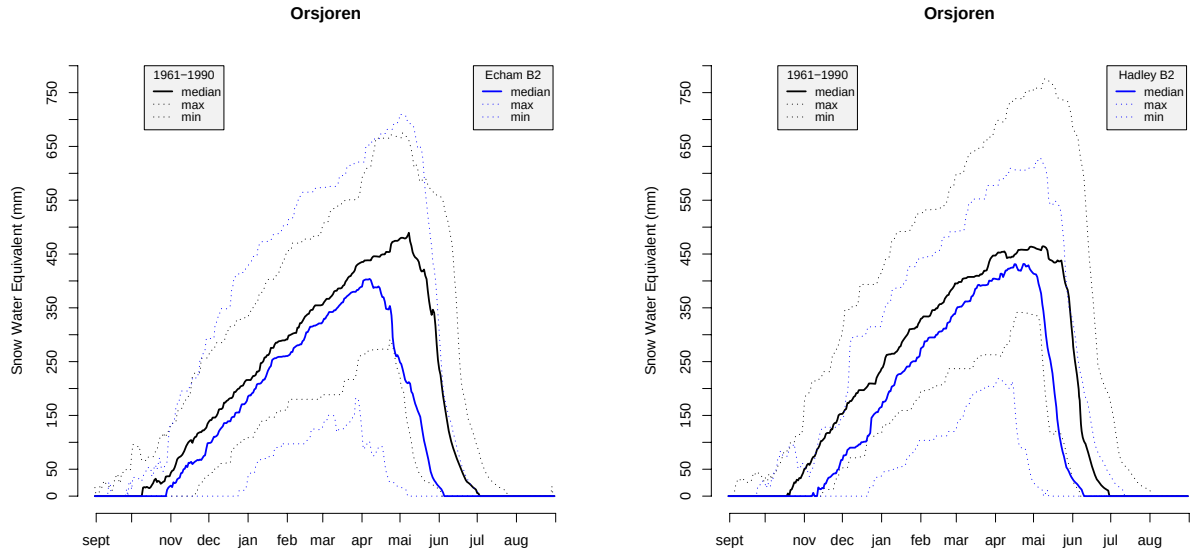

Figure 13: *Daily snow water equivalent: Orsjoren drainage basin*

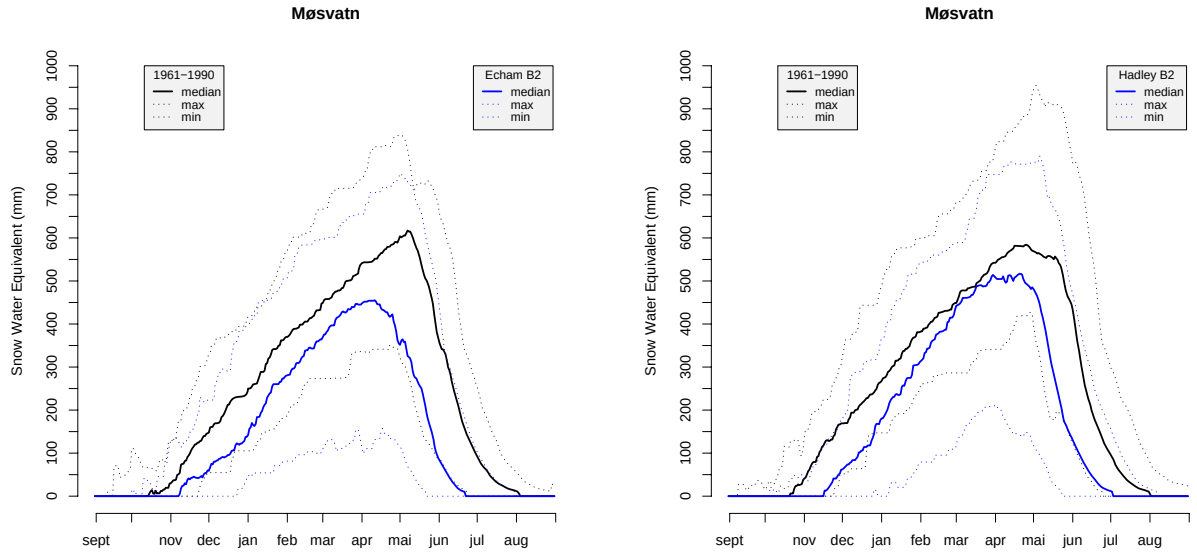

Figure 14: *Daily snow water equivalent: Møsvatn drainage basin*

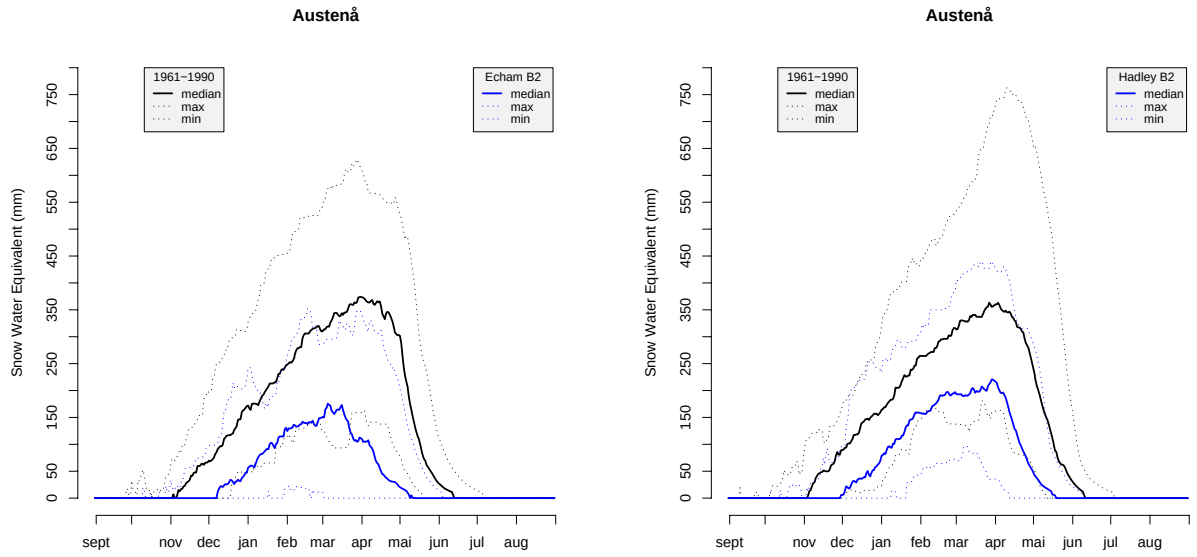

Figure 15: *Daily snow water equivalent: Austenå drainage basin*

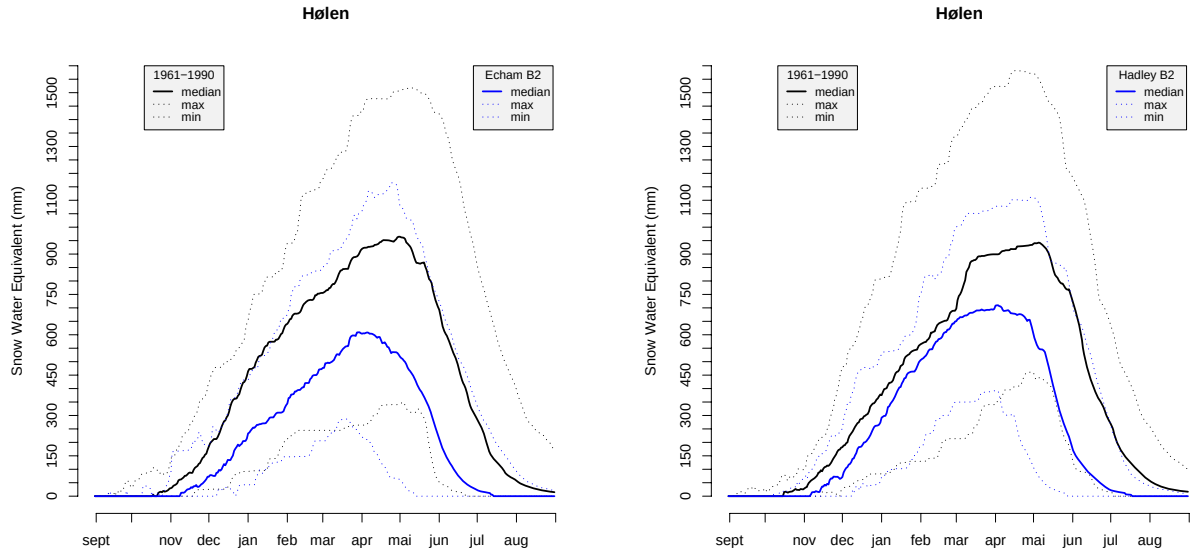

Figure 16: *Daily snow water equivalent: Hølen drainage basin*

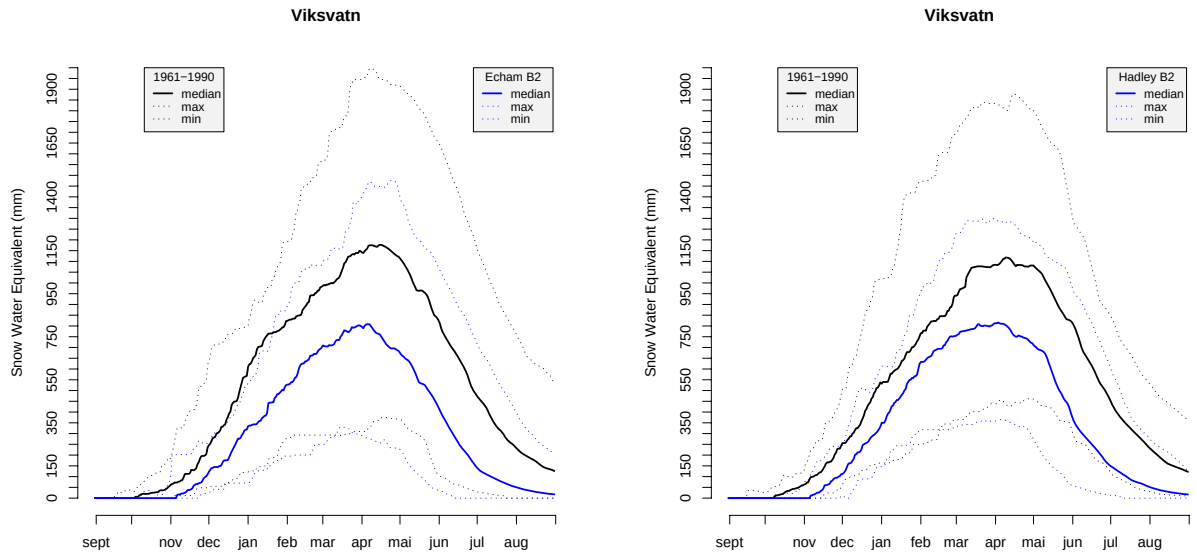

Figure 17: *Daily snow water equivalent: Viksvatn drainage basin*

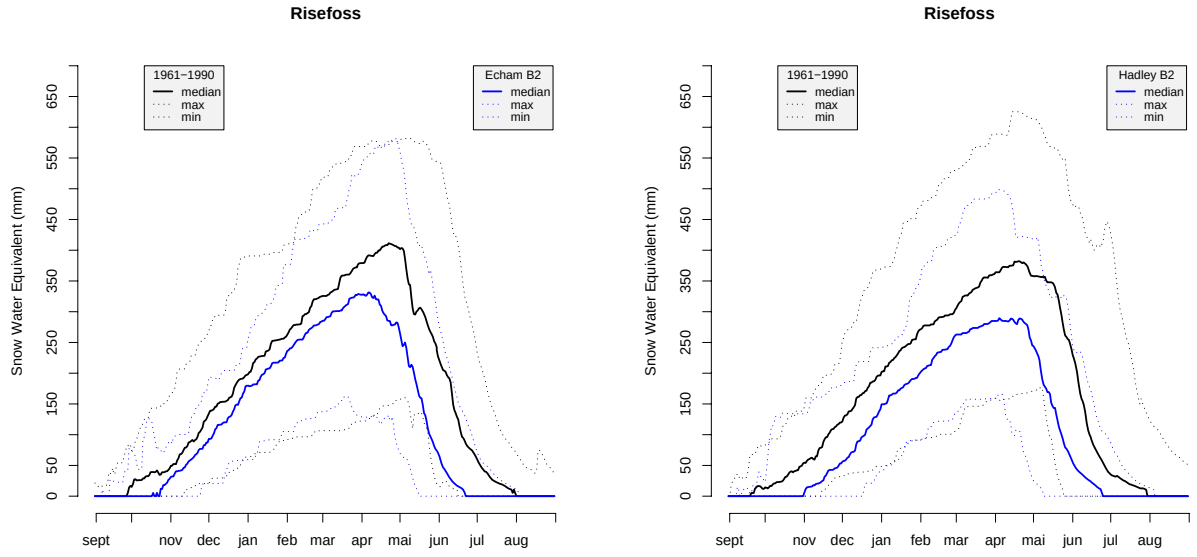

Figure 18: *Daily snow water equivalent: Risefoss drainage basin*

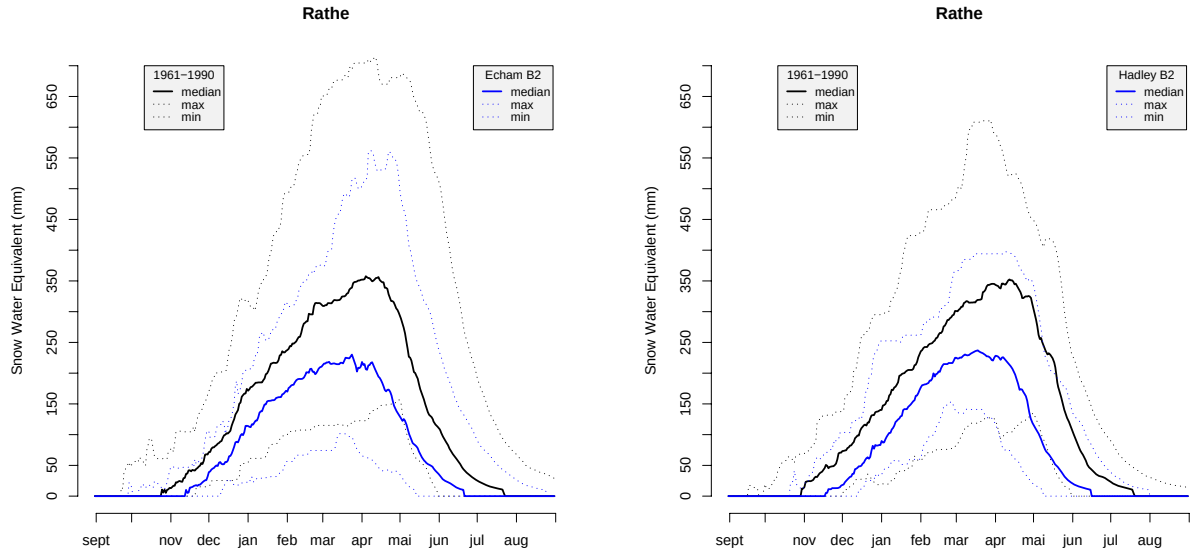

Figure 19: *Daily snow water equivalent: Rathe drainage basin*

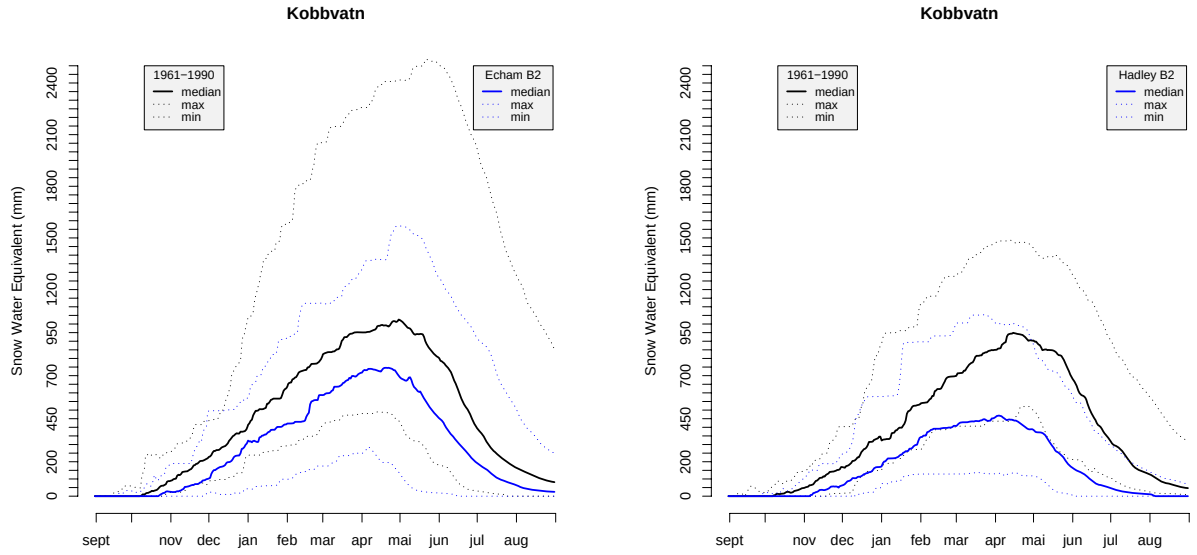

Figure 20: *Daily snow water equivalent: Kobbvatn drainage basin*

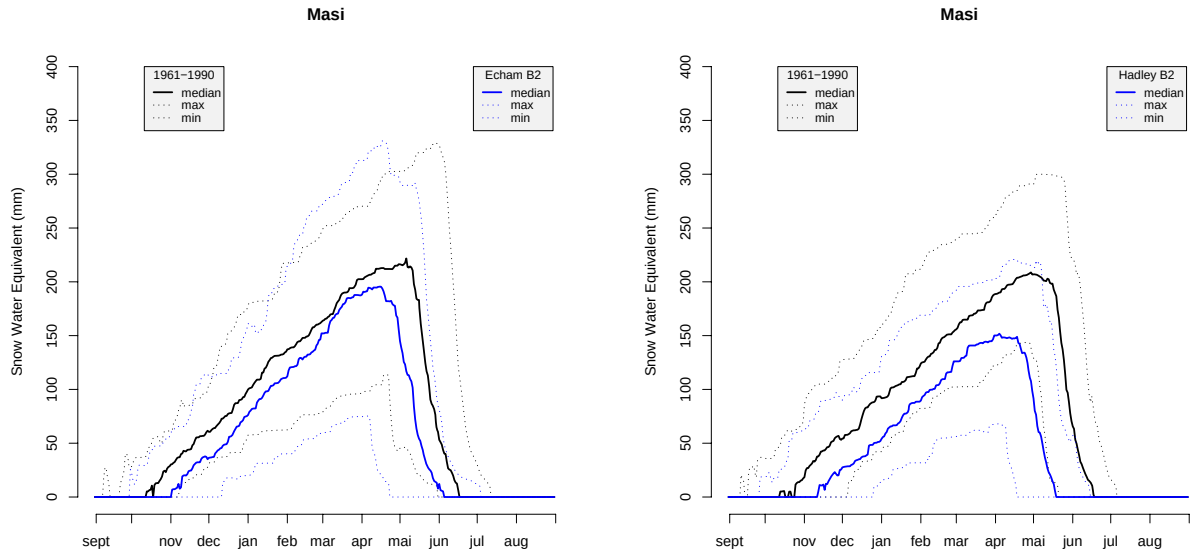

Figure 21: *Daily snow water equivalent: Masi drainage basin*

4.2 Changes in snow season duration

To study changes in the snow season duration, we have defined the term "permanent snow cover" as a period with more than 10 consecutive days where snow is present (snow water equivalent > 0 mm). Using this definition we were able to extract the start and the end of the snow season:

- First date of the first period with permanent snow cover.
- Last date of the last period with permanent snow cover.

Tabs. 5 and 6 show the first and the last date of permanent snow cover, derived from the median curves of data set A, B and C (Tabs. 1 and 2). For data sets B and C only the scenario period is included (dates are derived from the median curves presented in Figs. 10- 21). These tables provide a comparison of the snow cover duration observed during 1961-1990 and projected for future climate (2071-2100).

The date 31 August appears sometimes as the end of the snow season (Sjodalsvatn, Hølen, Viksvatn and Kobbvatn in Tab 6). This date corresponds to the last day of the hydrological year, when the GWB model resets the snow cover to zero. The reset is done because the model presumably overestimates the snow cover. The snow probably melts quicker than what is given by the model. The drainage basins, where this problem appears, either have glaciers present today or there are glaciers in the surrounding area. The model does not contain modules for converting accumulated snow to glacier ice.

Generally, these results show:

- that all drainage basins get at later start of the snow season: approximately 3-4 weeks later starting date, shifted from October/November to November/December.
- that almost all drainage basins get an earlier end of the snow season: varying from 1-7 weeks earlier ending date.

drainage basin	Observed 1961-1990	Hadley B2 2071-2100	Echam B2 2071-2100
Sjodalsvatn	23 Sept	31 Oct	21 Oct
Aursunden	21 Okt	12 Nov	4 nov
Knappom	14 Nov	9 Dec	11 Dec
Orsjoren	14 Oct	13 Nov	30 Oct
Møsvatn	13 Oct	18 Nov	9 Nov
Austenå	9 Nov	1 Dec	9 Dec
Hølen	11 Oct	7 Nov	10 Nov
Viksvatn	10 Oct	7 Nov	7 Nov
Risefoss	23 Sep	2 Nov	25 Oct
Rathe	30 Oct	19 Nov	14 Nov
Kobbvatn	13 Oct	7 Nov	24 Oct
Masi	20 Oct	13 Nov	3 Nov

Table 5: *First date of continuous snow cover, derived from the median curve. Present climate "Observed 1961-1990" is based on data set A (Tab. 1).*

drainage basin	Observed 1961-1990	Hadley B2 2071-2100	Echam B2 2071-2100
Sjodalsvatn	31 Aug*	22 Aug	11 Aug
Aursunden	4 Jul	1 Jun	3 Jun
Knappom	19 Mai	20 Apr	29 Mar
Orsjoren	5 Jul	10 Jun	5 Jun
Møsvatn	10 Aug	3 Jul	22 Jun
Austenå	5 Jun	19 May	9 May
Hølen	31 Aug*	18 Jul	14 Jul
Viksvatn	31 Aug*	31 Aug*	31 Aug*
Risefoss	16 Aug	25 Jun	22 Jun
Rathe	11 Jul	16 Jun	21 Jun
Kobbvatn	31 Aug*	5 Aug	31 Aug*
Masi	17 Jun	19 May	5 Jun

Table 6: *Last date of continuous snow cover, derived from the median curve. Present climate "Observed 1961-1990" is based on data set A (Tab. 1). *31 August is the last day of the hydrological year. The GWB resets the snow cover to zero to avoid accumulation of snow on glaciers as the model has no means of converting snow to glacier ice.*

4.3 Changes in maximum snow water equivalent

In addition to changes in snow season duration it is highly interesting to study changes in maximum snow water equivalent, as well as changes in time of year when maximum amounts of snow will occur. Using the same data sets (median curves) as described in Section 4.2 we derived these two snow variables:

- Maximum snow water equivalent.
- Date of maximum snow water equivalent.

The results show that there will be considerably less snow in all drainage basins in the period 2071-2100. Maximum snow water equivalent will be reduced with -10% to -70% compared to current climate (1961-1990). The date when maximum amounts of snow will occur is in many cases projected to shift from April/May to March/April, varying from 0-4 weeks earlier.

drainage basin	**Observed 1961-1990**	**Hadley B2 2071-2100**	**Echam B2 2071-2100**
Sjodalsvatn	5 May	22 Apr	22 Apr
Aursunden	1 May	4 Apr	25 Mar
Knappom	8 Apr	19 Mar	22 Feb
Orsjoren	22 Apr	24 Apr	8 Apr
Møsvatn	21 Apr	21 Apr	12 Apr
Austenå	10 Apr	30 Mar	6 Mar
Hølen	21 Apr	4 Apr	31 Mar
Viksvatn	6 Apr	4 Apr	6 Apr
Risefoss	1 May	5 Apr	7 Apr
Rathe	15 Apr	19 Mar	25 Mar
Kobbvatn	6 May	5 Apr	20 Apr
Masi	22 Apr	5 Apr	16 Apr

Table 7: *Date of maximum snow water equivalent derived from the median curves.*

drainage basin	**Observed 1961-1990**	**Hadley B2 2071-2100**		**Echam B2 2071-2100**	
	(mm)	(mm)	(%)	(mm)	(%)
Sjodalsvatn	756	634	-16	643	-15
Aursunden	413	294	-29	273	-34
Knappom	194	98	-49	59	-70
Orsjoren	495	431	-13	403	-19
Møsvatn	627	516	-18	455	-27
Austenå	369	220	-40	175	-53
Hølen	922	709	-23	609	-34
Viksvatn	1152	816	-29	808	-30
Risefoss	387	289	-25	331	-14
Rathe	410	237	-42	230	-44
Kobbvatn	922	467	-49	745	-19
Masi	214	151	-29	195	-9

Table 8: *Maximum snow water equivalent derived from the median curves. Projected change (%) from current to future climate is also included.*

4.4 Summary of changes in snow water equivalent for all drainage basins

In this section we summarize the main results for the 12 drainage basins by presenting two graphs, one for HadAm3-B2 and one for ECHAM4/OPYC3-B2. The graphs contain one curve for each drainage basin, calculated by subtracting the median curves in Figs. 10- 21.

An interesting trend is observed for several of the drainage basins (e.g. Sjodalsvatn, Møsvatn, Risefoss, Hølen and Orsjoren). This trend is more distinct with data from HadAm3-B2 (Fig. 22) as compared to data from ECHAM4/OPY-B2 (Fig.. 23). Less snow is projected during October, November and December, because the accumulation season starts later than before. Furthermore, this deviation is reduced during the period from December to March because of increased winter precipitation. In March the projected snow accumulation seems almost to catch up with the current snow accumulation. A huge deviation is again projected during May and June (e.g. Kobbvatn, Viksvatn, Hølen, Orsjoren, Sjodalsvatn, Møsvatn). This is related to an earlier start of the snow melt season.

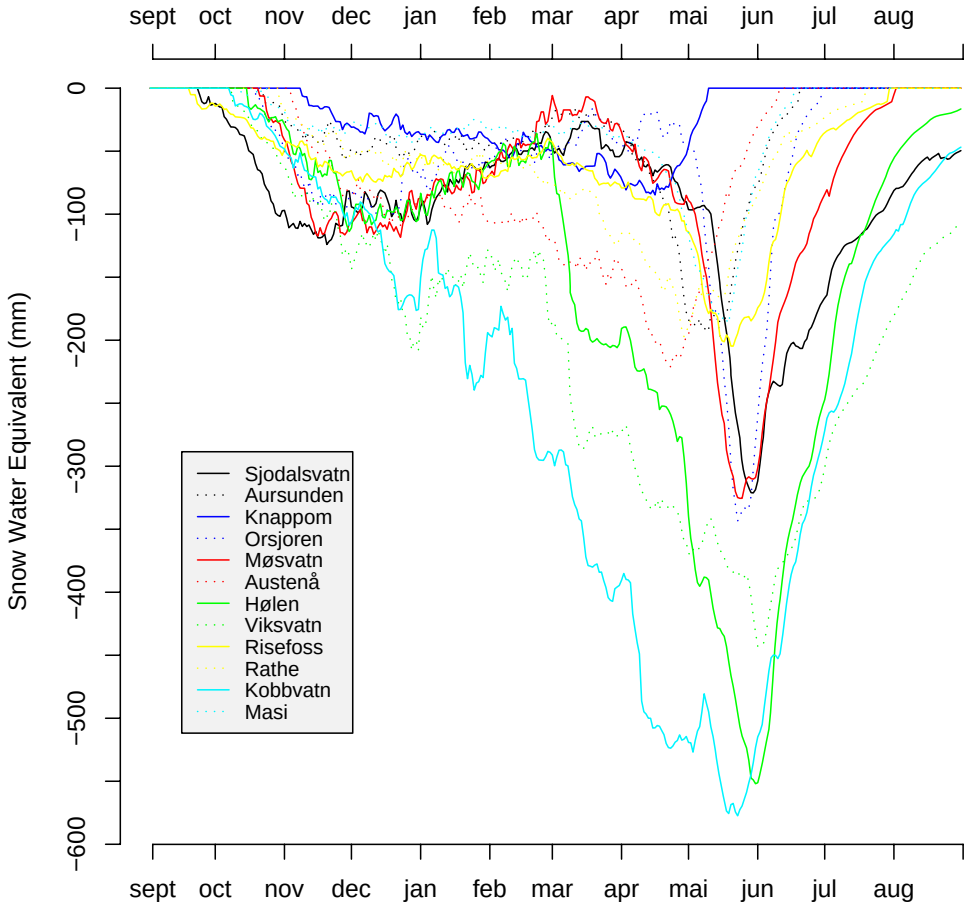

Figure 22: *Comparison of 12 drainage basins showing reduced snow water equivalent from the control period (1961-1990) to the scenario period (2071-2100), modeled with the HadAm3 climate model.*

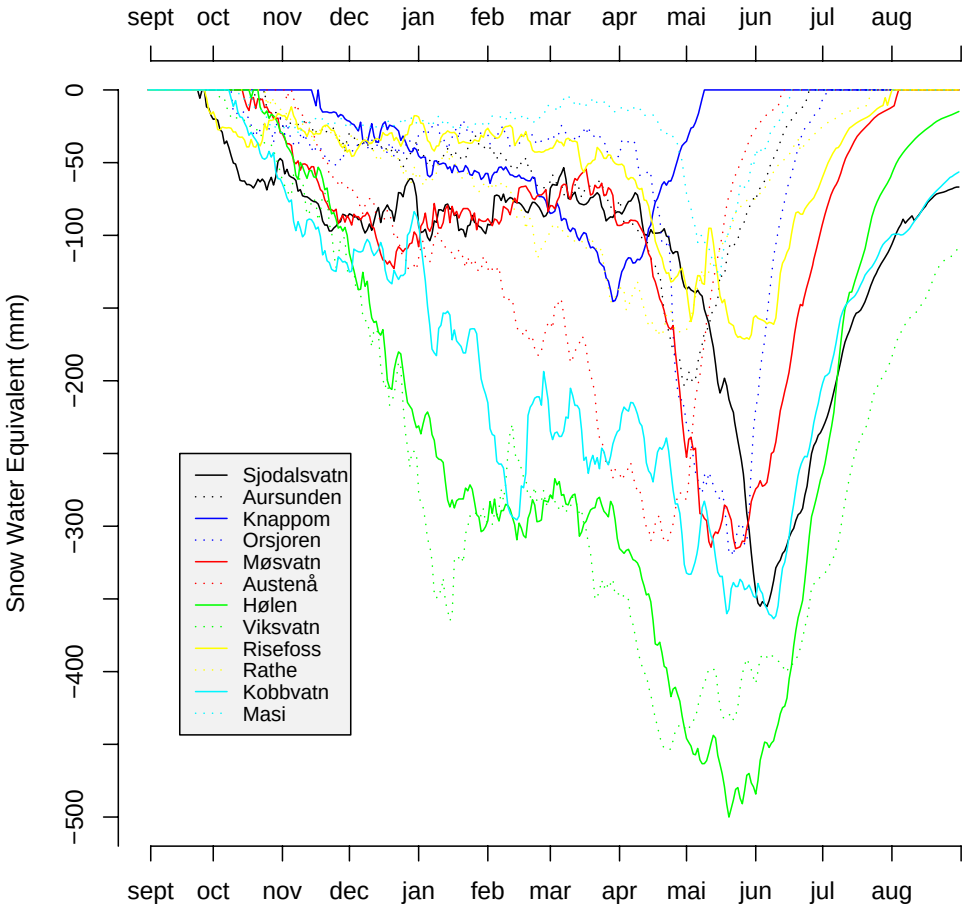

Figure 23: *Comparison of 12 drainage basins showing reduced snow water equivalent from the control period (1961-1990) to the scenario period (2071-2100), modeled with the ECHAM4/OPYC3 climate model*

5 Discussion

5.1 Uncertainties in climate modelling

The modelling of climate involves a number of uncertainties as the understanding of the entire climate system with all relevant processes is incomplete. Furthermore, climate models cannot possibly account for every process at the very smallest scales explicitly. Hence, AOGCMs must approximate descriptions of a large number of processes that take place on a spatial scale unresolved by the model grid boxes. For instance, the description of cloud processes, ocean currents, and vapour/energy exchange between the atmosphere and the surface may vary with the location and can only be described by a general approximation. A variety of climate models exist and it has been shown that each model can give a different picture of the climate evolution (Cubasch et al., 2001).

Benestad (2000) noted that the climate model spin-up process is important for the description of the local climatic evolution, and that there were regional differences between four simulations done with the HadCM2 model for different initial conditions. These differences were regarded as a result of the non-linear chaotic behaviour of climate, and hence part of the unpredictable natural variability (Benestad, 2001). It is also evident that these natural fluctuations contaminate the climate change analysis such as for 30-year long time slices. Benestad (2003) argued that part of the natural variations are "externally forced", by for instance volcanoes, solar activity or landscape changes, and will therefore not be captured by climate models only prescribed with emission data.

5.2 Uncertainties in dynamical downscaling

Regional climate models (RCMs) are promising tools to derive climate change scenarios on spatial scales that are represented too coarse by the AOGCMs. RCM simulations are frequently used as input data for climate impact studies (Wood et al., 2004; Bronstert, 2004) which require the representations of the present climate to be realistically reproduced by the RCM especially with respect to the variability, change and impacts on extreme events. The statistics of precipitation estimates (mean, wet-day frequency, precipitation intensity and quantiles of the frequency distribution), based on five different RCMs, are analysed by Frei et al. (2003). They found considerable biases when comparing the statistics. The time resolution of archived output from dynamically downscaled scenarios is typically on a 6 hourly basis. The spatial resolution (typically 50 km x 50 km), however, is too coarse to be representative locally. The terrain in the regional climate models is smoothened, the sites elevation is thus wrongly represented, and the frequency of days with precipitation is overestimated (Charles et al., 1999). Observed climate of specific sites, especially in areas with complex topography, is therefore not well reproduced. The AOGCM is initially developed to capture the overall regional weather pattern of an area. Interpolation of temperature and precipitation data from RCMs to at site locations therefore requires special attention. It is also important to note that the representation of a parameter in RCM may be either a point value or a mean value for a given grid box volume, and which of these representations are used in the model formulation may not always be obvious when bringing together a large variety of different models describing a range of processes over different scales.

5.3 Uncertainties in hydrological modelling

The hydrological model represents a simplified description of the hydrological processes governing the streamflow generation in a basin. Furthermore, the model utilises data from a limited number of climate stations to estimate the streamflow as well as other water balance elements. Daily temperature and precipitation data are assigned to grid-cells of 1 km^2 based on the three closest climate stations taking into account differences in altitudes and land use. The simplified description of the governing processes will introduce uncertainties in the simulated data. The uncertainty in the meteorological data driving the model both in terms of values and representativity of the data is probably a more important contribution to the uncertainties in the simulated streamflow and other water balance elements.

The calibration of the model results in mostly good agreement between observed and simulated streamflow in the calibration period as shown in Fig. 24. The average bias in annual means is -0.44% for

22 basins. The average bias is 3.49% in the winter, 1.34% in the spring, -0.70% in the summer and 1.9% in the autumn. The winter streamflow is quite low in some of the basins, and the observations are also most unreliable at this time of the year. This explains the larger errors in the winter season. The model seems to capture the variability fairly well in most basins. The largest errors stem from the use of less representative precipitation data.

An example of simulated and observed time-series of snow water equivalent is provided in Fig. 25. The figure shows the snow pillow at Vauldalen in the Aursunden catchment.

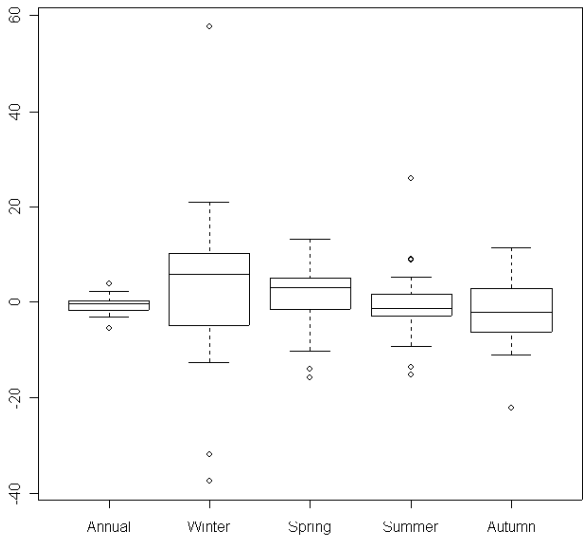

Figure 24: *Percentage differences between observed and simulated streamflow in the calibration period for 22 basins, shown as a Box whiskers diagram. 1: Annual, 2: Winter, 3: Spring, 4: Summer, 5: Autumn means.*

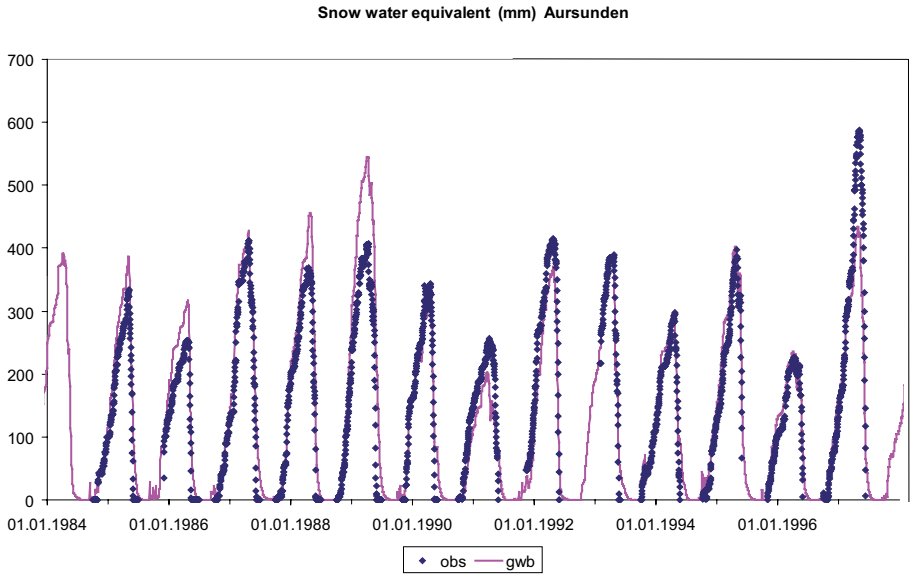

Figure 25: *Observed and simulated snow water equivalent (mm) in the Aursunden catchment for period 1984-1997.*

6 Summary

This report presents projected changes in snow conditions in Norway. Possible changes from present climate (1961-1990) to future climate (2071-2100) are described. Projected air temperature and precipitation data from two climate models (HadAm3 and ECHAM4/OPYC3) run with the B2 emission scenario were dynamically downscaled using the regional climate model HIRHAM, and also locally adjusted to stations in Norway. The Gridded Water Balance model was run using these daily data sets. Snow water equivalent, which is reported in this study, is one of the output variables.

Given the projected air temperature and precipitation data for 2071-2100, the snow conditions might change in the following way, as compared to present climate (1961-1990):

- Mean annual maximum snow water equivalent is projected to decrease almost everywhere in Norway.
- Largest relative changes are expected to occur in some of the outermost areas on the west coast of Norway (80-100% decrease), but in these areas the snow amounts are small even under the present climate (<40 mm mean annual maximum snow water equivalent). A north-south zone around the fjords in West-Norway and North-Norway might get decreases up to 60-80%.
- Smallest relative changes (0-19% decrease) are projected in mountainous areas in South Norway, as well as inner regions of North Norway (Finmarksvidda).
- The duration of the snow season is expected to be shorter almost everywhere in Norway. Generally, the decrease gets smaller with increasing altitude and distance from the coast.
- The start of the snow accumulation season is projected approximately 3-4 weeks later than in the present climate (12 drainage basins are analyzed).
- The snow melt season starts earlier, leading to an earlier end of the snow season. In the 12 studied drainage basins the ending date is 1-7 weeks earlier than in the present climate.
- Maximum amount of snow is projected to shift from April/May to March/April, varying from 0-4 weeks earlier (12 drainage basins are analyzed).
- In extreme years the maximum snow water equivalent might be higher than today in a few high altitude or northern drainage basins.

There are many sources of uncertainties in the scenarios, in the climate modelling, the downscaling to climate stations and in the hydrological modelling. The uncertainty caused by the hydrological model are of less importance than the uncertainties caused by the representativity of the meteorological data driving the model.

References

Beldring, S., Engeland, K., Roald, L. A., Sælthun, N. R., and Voksø, A. (2003). Estimation of parameters in a distributed precipitation-runoff model for Norway. *Hydrology and Earth System Sciences*, 7(3):304–316.

Beldring, S., Roald, L. A., and Voksø, A. (2002). Avrenningskart for Norge. Årsmiddelverdier for avrenning. NVE Document No. 2, Norwegian Water Resources and Energy Administration, Oslo, Norway.

Benestad, R. E. (2000). Future climate scenarios for Norway based on empirical downscaling and inferred directly from AOGCM results. Technical Report 23/00, Meteorological Institute, Oslo, Norway.

Benestad, R. E. (2001). The cause of warming over Norway in the ECHAM4/OPYC3 GHG integration. *International Journal of Climatatology*, 21(3):371–387.

Benestad, R. E. (2002). Empirically downscaled multi-model ensemble temperature and precipitation scenarios for Norway. *Journal of Climate*, 15:3008–3027.

Benestad, R. E. (2003). What can present climate models tell us about climate change? *Climate Change*, 59(3):311–331.

Bergström, S. (1976). Development and application of a conceptual runoff model for Scandinavian catchments. SMHI report RH07, Sweedish Meteorological and Hydrological Institute, Norrköping, Sweeden.

Bjørge, D., Haugen, J. E., and Nordeng, T. E. (2000). Future climate in Norway. Dynamical downscaling experiments within the RegClim project. Report no. 103, Meteorological Institute, Oslo, Norway.

Bronstert, A. (2004). Rainfall-runoff modelling for assessing impacts of climate and land-use change. *Hydrological Processes*, 18:567–570.

Charles, S., Bates, B. C., Whetton, P. H., and Hughes, J. P. (1999). Validation of downscaling models for changed climate conditions: Case study of southwestern Australia. *Climate Research*, 12:1–14.

Cubasch, U., Meehl, G. A., Boer, G. J., Stouffer, R. J., Dix, M., Noda, A., Senior, C. A., Raper, S., and S., Y. K. (2001). Projections of future climate change. In *Climate change 2001: The scientific basis. Contribution of Working Group I to the third assessment report of the Intergovernmental Panel on Climate Change*, pages 583–638. Cambridge University Press, Cambridge, Great Britain.

Doherty, J., Brebber, L., and Whyte, P. (1998). PEST. Model independent parameter estimation. User manual, 2nd edition, Watermark Numerical Computing, Brisbane, Australia.

Engen-Skaugen, T. (2002). Refinement of dynamically downscaled precipitation and temperature scenarios. met.no report no. 15, Meteorological Institute, Oslo, Norway.

Engen-Skaugen, T., Hanssen-Bauer, I., and Førland, E. J. (2002). Adjustment of dynamically downscaled temperature and precipitation data in norway. met.no report no. 20, Meteorological Institute, Oslo, Norway.

Folland, C. K., Karl, T. R., Christy, J. R., Clarke, R. A., Gruza, G. V., Jouzel, J., Mann, M. E., Oerlemans, J., Salinger, M. J., and Wang, S. W. (2001). Observed climate variability and change. In *Climate change 2001: The scientific basis. Contribution of Working Group I to the third assessment report of the Intergovernmental Panel on Climate Change*. Cambridge University Press, UK & USA.

Frei, C., Christensen, J. H., Déqué, M., Jacob, D., Jones, R. G., and Vidale, P. L. (2003). Daily precipitation statistics in regional climate models: Evaluation and intercomparison for the European Alps. *Journal of Geophysical Resarch-Atmospheres*, 108(D3-4124).

Gordon, C., Cooper, C., Senior, C. A., Banks, H., Gregory, J. M., Johns, T. C., Mitchell, J. B. F., and Wood, R. A. (2000). The simulation of SST, sea ice extents and ocean heat transport in a version of the Hadley Centre coupled model without flux adjustments. *Climate Dynamics*, 616:147–168.

Gottschalk, L., Beldring, S., Engeland, K., Tallaksen, L., Sælthun, N. R., Kolberg, S., and Motovilov, Y. (2001). Regional/macroscale hydrological modelling: a Scandinavian experience. *Hydrological Sciences Journal*, 46:963–982.

Haugen, J. E. and Iversen, T. (2005). Response in daily precipitation and wind speed extremes from HIRHAM downscaling of SRES B2 scenarios. In *RegClim General Technical Report No. 8*, pages 35–50.

Matheussen, B., Kirschbaum, R. L., Goodman, I. A., O'Donnel, G. M., and Lettenmaier, D. (2000). Effects of land cover change on streamflow in the interior Columbia river basin (USA and Canada). *Hydrological Processes*, 14:867–885.

Roald, L. A., Beldring, S., Engen Skaugen, T., Førland, E. J., and Benestad, R. (2006). Climate change impacts on streamflow in Norway. NVE Consultancy report A no. 1-2006, Norwegian Water Resources and Energy Directorate, Oslo, Norway.

Roeckner, E., Bengtsson, L., Feichter, j., Lelieveld, J., and Rodhe, H. (1999). Transient climate change simulations with a coupled atmosphere-ocean GCM including the tropospheric suphur cycle. *Journal of Climate*, 12:3004–3032.

Sælthun, N. R. (1996). The Nordic HBV model. NVE Report No. 7, Norwegian Water Resources and Energy Administration, Oslo, Norway.

Weglarczyk, S. (1998). The interdependence and applicability of some statistical quality measures for hydrological models. *Journal of Hydrology*, 206:98–103.

Wood, A. W., Leung, L. R., Sridhar, V., and lettenmaier, D. P. (2004). Hydrologic implications of dynamical and statistical approaches to downscaling climate model outputs. *Climatic Change*, 62(1-3):189–216.